

# Theoretical and experimental study of particle trajectories for nonlinear water waves propagating on a sloping bottom

BY YANG-YIH CHEN<sup>1,2</sup>, MENG-SYUE LI<sup>1</sup>, HUNG-CHU HSU<sup>3,\*</sup> AND  
CHIU-ON NG<sup>4</sup>

<sup>1</sup>*Department of Marine Environment and Engineering, National Sun Yat-sen University, Kaohsiung 80424, Taiwan*

<sup>2</sup>*Department of Hydraulic and Ocean Engineering, National Cheng Kung University, Tainan 70955, Taiwan*

<sup>3</sup>*Tainan Hydraulics Laboratory, National Cheng Kung University, Tainan 70101, Taiwan*

<sup>4</sup>*Department of Mechanical Engineering, The University of Hong Kong, Hong Kong, People's Republic of China*

A third-order asymptotic solution in Lagrangian description for nonlinear water waves propagating over a sloping beach is derived. The particle trajectories are obtained as a function of the nonlinear ordering parameter  $\epsilon$  and the bottom slope  $\alpha$  to the third order of perturbation. A new relationship between the wave velocity and the motions of particles at the free surface profile in the waves propagating on the sloping bottom is also determined directly in the complete Lagrangian framework. This solution enables the description of wave shoaling in the direction of wave propagation from deep to shallow water, as well as the successive deformation of wave profiles and water particle trajectories prior to breaking. A series of experiments are conducted to investigate the particle trajectories of nonlinear water waves propagating over a sloping bottom. It is shown that the present third-order asymptotic solution agrees very well with the experiments.

**Keywords:** Lagrangian; sloping bottom; particle trajectory; wave velocity relation; wave breaking

## 1. Introduction

In the process of a wave propagating from deep to shallow water, the wave will deform and eventually break. The wave changes in height and its profile becomes asymmetrical during the process of shoaling. In this connection, many researchers have paid much attention to solving the wave transformation on sloping bottoms. Moreover, it is also very important for the tsunami issue as discussed by Segur [1] and Constantin & Johnson [2]. However, since the sloping bottom was approximated by a large number of steps, the effects of the bottom

\*Author for correspondence (hchs@thl.ncku.edu.tw).

One contribution of 13 to a Theme Issue 'Nonlinear water waves'.

slope could not be fully explained in many models. Biesel [3] suggested a plausible approximation method to account for the normal incident waves propagating on a sloping plane where the bottom slope was first considered in the velocity potential as a perturbation parameter. Chen & Tang [4] modified Biesel's [3] theoretical model and obtained a linear solution to the first order of the bottom slope. For nonlinear waves on a beach, Carrier & Greenspan [5] gave an analytical solution for the shallow water wave motion of finite-amplitude, non-breaking waves on a beach of constant slope. Chu & Mei [6] and Liu & Dingemans [7] presented perturbation solutions for weakly nonlinear waves propagating over an uneven bottom. Chen *et al.* [8] derived a fourth-order asymptotic solution of nonlinear water waves propagating normally towards a mild beach. Chen *et al.* [8] used the transformation from Eulerian to Lagrangian coordinates to calculate the water particle motion up to the second order, by which the profile of a shoaling wave sequence until the breaking point can be evaluated. However, a straightforward expansion of the Eulerian solution of Stokes waves up to the third order cannot be transformed into the corresponding Lagrangian solution. Chen & Hsu [9] presented a modified Euler–Lagrange transformation method to obtain the third-order trajectory solution in a Lagrangian form for the water particles in nonlinear water waves. Unlike an Eulerian surface, which is given as an implicit function, a Lagrangian form is expressed through a parametric representation of particle motion. Hence, the Lagrangian description is more appropriate for the free surface motion, whereas this unique feature cannot be represented by the classical Eulerian solutions [3,8,10–17].

The first water wave theory in Lagrangian coordinates was obtained by Gerstner [18] who assumed the flow possesses non-constant vorticity in infinite depth. Miche [19] proposed a perturbation method for Lagrangian solution to the second order for a gravity wave motion. Pierson [20] also applied perturbation expansion to water wave problems with Lagrangian formulae and obtained a first-order Lagrangian solution. Buldakov *et al.* [16] developed a Lagrangian asymptotic formulation up to the fifth order for nonlinear water waves in deep water. Recently, for travelling waves in irrotational flow over a flat bed, the general features of the particle paths have been obtained without the assumption of small amplitude (necessary for a power-series approach) by Constantin [21]; the particle trajectories in solitary water waves have also been obtained by Constantin & Escher [22]; and Constantin & Strauss [23] have extended the work to describe the pressure beneath a Stokes wave. Additionally, Constantin & Escher [24] have further exposed the analyticity of periodic travelling free surface water waves with vorticity. Chen & Hsu [9] obtained a third-order solution for irrotational finite amplitude standing waves in Lagrangian coordinates. The particle path is similar to Ehrnström & Wahlen [25]. Hsu *et al.* [26] derived a Lagrangian asymptotic solution up to the second order for short-crested waves. Asymptotic solutions up to the fifth order which describe irrotational finite amplitude progressive gravity water waves were recently derived in Lagrangian description by Chen *et al.* [27]. All the theories mentioned above are limited to the condition of uniform water depth. To date, only a few analytical solutions have been derived for wave transformation on a planar beach in Lagrangian coordinates. Among them, Sanderson [28] obtained a second-order solution in a uniformly stratified fluid with a small bottom slope in a Lagrangian system. Constantin [29] considered the Lagrangian solution for edge waves on a sloping beach. Chen & Huang [30]

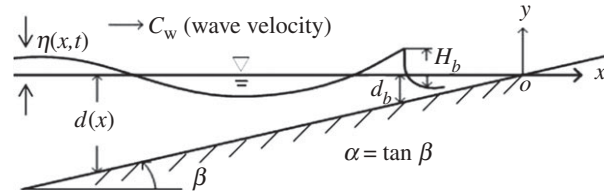


Figure 1. Definition sketch for surface-wave propagation on a uniformly sloping bottom.

derived a linear Lagrangian solution in terms of beach slope  $\alpha$  to the second order for a progressive wave propagating over a gentle plane slope, while Kapinski [31] studied the run-up of a long wave over a uniform sloping bottom in Lagrangian description.

The purpose of this paper is to develop a nonlinear solution for surface waves propagating over a sloping bottom in a Lagrangian description and to compare the theory with a series of experiments. In order to examine the effect of a sloping bottom and wave steepness on surface waves, a perturbation expansion is used to derive an expression for the particle trajectories in terms of wave steepness  $\epsilon$  and the bottom slope  $\alpha$  to the third power. The asymptotic solutions for physical quantities related to the wave motion are then obtained up to the third order. Finally, to validate the accuracy of the analytical results, a series of laboratory experiments are performed. The Lagrangian properties of particle trajectories are shown to agree with the experimental data very well.

### 2. Formulation of the problem

Consider a two-dimensional monochromatic wave propagating on a uniform gentle slope without refraction as shown in figure 1. The negative  $x$ -axis is outward to the sea from the still water level (SWL) shoreline, while the  $y$ -axis is taken positive vertically upward from the SWL, and the sea bottom is at  $y = -d = \alpha x_0$ , in which  $\alpha$  denotes the bottom slope.

The fluid motion in the Lagrangian representation is described by keeping track of individual fluid particles. For two-dimensional flow, a fluid particle is identified by the horizontal and vertical parameters  $(x_0, y_0)$  known as Lagrangian labels. Then fluid motion is described by a set of trajectories  $x(x_0, y_0, t)$  and  $y(x_0, y_0, t)$ , where  $x$  and  $y$  are the Cartesian coordinates. The dependent variables  $x$  and  $y$  denote the position of any particle at time  $t$  and are functions of the independent variables  $x_0, y_0$  and  $t$ . In a system of Lagrangian description, the governing equations and boundary conditions for two-dimensional irrotational free-surface flow are summarized as follows:

$$J = \frac{\partial(x, y)}{\partial(x_0, y_0)} = x_{x_0} y_{y_0} - x_{y_0} y_{x_0} = 1, \tag{2.1}$$

$$x_{x_0 t} y_{y_0} - x_{y_0 t} y_{x_0} + x_{x_0} y_{y_0 t} - x_{y_0} y_{x_0 t} = \frac{\partial(x_t, y)}{\partial(x_0, y_0)} + \frac{\partial(x, y_t)}{\partial(x_0, y_0)} = 0, \tag{2.2}$$

$$x_{x_0 t} x_{y_0} - x_{y_0 t} x_{x_0} + y_{x_0 t} y_{y_0} - y_{y_0 t} y_{x_0} = \frac{\partial(x_t, x)}{\partial(x_0, y_0)} + \frac{\partial(y_t, y)}{\partial(x_0, y_0)} = 0, \tag{2.3}$$

$$\frac{\partial \phi}{\partial x_0} = x_t x_{x_0} + y_t y_{x_0}, \quad \frac{\partial \phi}{\partial y_0} = x_t x_{y_0} + y_t y_{y_0} \tag{2.4}$$

and 
$$\frac{P}{\rho} = -\frac{\partial \phi}{\partial t} - gy + \frac{1}{2}(x_t^2 + y_t^2). \tag{2.5}$$

In equations (2.1)–(2.5), subscripts  $x_0$ ,  $y_0$  and  $t$  denote partial differentiation with respect to the specified variable,  $P(x_0, y_0, t)$  is water pressure and  $\phi(x_0, y_0, t)$  is a velocity potential function in Lagrangian system. Except for equations (2.4) and (2.5) by Chen [32], the fundamental physical relationships defining the equations above have been derived previously [19,20,33,34]. Equation (2.1) is the continuity equation that sets the invariant condition on the volume of a Lagrangian particle and  $y_0 = 0$  is the vertical label marked for a particle at free surface; equation (2.2) is the differentiation of equation (2.1) with respect to time. Equations (2.3) and (2.4) govern the irrotational flow condition and define the corresponding Lagrangian velocity potential, respectively. Equation (2.5) is the Bernoulli equation for irrotational flow in Lagrangian description.

The wave motion has to satisfy a number of boundary conditions at the bottom and on the free water surface.

- On an immovable and impermeable sloping plane with an inclination to the horizon, the no-flux bottom boundary condition gives

$$y_t - \alpha x_t = 0 \quad \text{and} \quad y = y_0 = -d = \alpha x_0. \tag{2.6}$$

- The dynamic boundary condition of zero pressure at the free surface is

$$P = 0, \quad y_0 = 0. \tag{2.7}$$

- A time-averaged and stationary mass flux conservation condition is required: as waves propagate towards the beach, a horizontal hydrostatic pressure gradient to balance the radiation stress of the progressive wave will produce a return flow and a boundary condition should be imposed. The additional condition usually employed is the condition of time-averaged mass flux conservation. This condition is necessary for the uniqueness of the solution and requires that at any cross section of the  $x$ - $y$  plane, the time-averaged mass flux should vanish [8,35,36]

$$y \text{ direction: } \frac{1}{T} \int_0^T \int_{-d}^0 v \, dy_0 \, dt = \frac{1}{T} \int_0^T \int_{-d}^0 y_t \, dy_0 \, dt = 0 \tag{2.8}$$

$$\begin{aligned} x \text{ direction: } & \frac{1}{T} \int_0^T \int_{-d}^0 u \, dy_0 \, dt = \frac{1}{T} \int_0^T \int_{-d}^0 x_t \, dy_0 \, dt \\ & - \frac{U(\alpha)}{T} \int_0^T \int_{-d_0}^0 x_t^c \, dy_0 \, dt = \overline{\int_{-d}^0 u \, dy_0} \\ & - U(\alpha) \overline{\int_{-d_0}^0 u^c \, dy_0} = 0, \quad U(\alpha) = \begin{cases} 0, & \alpha \neq 0, \\ 1, & \alpha = 0. \end{cases} \end{aligned} \tag{2.9}$$

Both the superscript  $c$  and the subscript 0 express the physical quantity at  $x \rightarrow -\infty$ . Because of the nonlinear effect, waves over constant depth induce a net flux of water. Thus, a constant depth streaming term is introduced in (2.9) which is adjusted by a unit function  $U(\alpha)$  to ensure that it can be reduced to the constant depth condition when the bottom slope is equal to zero.

### 3. Asymptotic solutions

To solve equations (2.1)–(2.9), it is assumed that relevant physical quantities can be expanded as a double power series in terms of the bottom slope  $\alpha$  and nonlinear parameter  $\varepsilon$ . Thus, the particle displacements  $x$  and  $y$ , the potential function  $\phi$ , wave pressure  $P$ , wavenumber  $k$  and Lagrangian wave frequency  $\sigma$  can be obtained as the following:

$$\begin{aligned} x &= x_0 + \sum_{m=0}^{\infty} \sum_{n=0}^{\infty} \varepsilon^m \alpha^n [f_{m,n}(x_0, y_0, \sigma t) + f'_{m,n}(x_0, y_0, \sigma_{0,0} t)] \\ &= x_0 + \sum_{m=0}^{\infty} \sum_{n=0}^{\infty} \varepsilon^m \alpha^n [A_{m,n,i} F_{m,n,i}(S) + A'_{m,n,i} F'_{m,n,i}(S)], \end{aligned} \quad (3.1)$$

$$\begin{aligned} y &= y_0 + \sum_{m=0}^{\infty} \sum_{n=0}^{\infty} \varepsilon^m \alpha^n [g_{m,n}(x_0, y_0, \sigma t) + g'_{m,n}(x_0, y_0, \sigma_{0,0} t)] \\ &= y_0 + \sum_{m=0}^{\infty} \sum_{n=0}^{\infty} \varepsilon^m \alpha^n [B_{m,n,i} G_{m,n,i}(S) + B'_{m,n,i} G'_{m,n,i}(S)], \end{aligned} \quad (3.2)$$

$$\begin{aligned} \phi &= \sum_{m=0}^{\infty} \sum_{n=0}^{\infty} \varepsilon^m \alpha^n \left[ \phi_{m,n}(x_0, y_0, \sigma t) + \phi'_{m,n}(\sigma_{0,0} t) + \int M_{m,n,0}(x_0, \sigma_{0,0} t) dx_0 \right] \\ &= \sum_{m=0}^{\infty} \sum_{n=0}^{\infty} \varepsilon^m \alpha^n \left[ \phi_{m,n,i} F_{m,n,i}(S) + \phi'_{m,n}(\sigma_{0,0} t) + \int M_{m,n,0}(x_0, \sigma_{0,0} t) dx_0 \right], \end{aligned} \quad (3.3)$$

$$P = -\rho g y_0 + \sum_{m=0}^{\infty} \sum_{n=0}^{\infty} \varepsilon^m \alpha^n P_{m,n}(x_0, y_0, \sigma t), \quad (3.4)$$

$$k = \sum_{m=0}^{\infty} \sum_{n=0}^{\infty} \varepsilon^m \alpha^n k_{m,n}(x_0, y_0) \quad (3.5)$$

$$\text{and } \sigma = \sum_{m=0}^{\infty} \varepsilon^m \alpha^n \sigma_{m,n}(x_0, y_0), \quad (3.6)$$

where  $S$  is the phase function  $S = \int k dx_0 - \sigma t$ ,  $x(x_0, y_0, t)$  and  $y(x_0, y_0, t)$  are the particle displacements and the Lagrangian variable  $(x_0, y_0)$  are any two characteristic parameters,  $\varepsilon$  is the nonlinear ordering parameter characterizing the wave steepness and  $M_{m,n,0}$  is the return flow.  $\sigma = 2\pi/T$  is the angular frequency of the particle motion or the Lagrangian angular frequency for a particle reappearing

at the same phase, where  $T$  is the period of particle motion. For a relatively gentle bottom slope  $\alpha$ , it may be assumed that the  $q$ -th differentiations of  $A_{m,n,i}$ ,  $A'_{m,n,i}$ ,  $B_{m,n,i}$ ,  $B'_{m,n,i}$ ,  $\phi_{m,n,i}$ ,  $M_{m,n,0}$  and  $k_{m,n}$  with respect to  $x_0$  are in the order of  $\alpha^q$ :

$$\left( \frac{d^q k_{m,n}}{dx_0^q}, \frac{\partial^q M_{m,n,0}}{\partial x_0^q}, \frac{d^q A_{m,n,i}}{dx_0^q}, \frac{d^q A'_{m,n,i}}{dx_0^q}, \frac{d^q B_{m,n,i}}{dx_0^q}, \frac{d^q B'_{m,n,i}}{dx_0^q}, \frac{d^q \phi_{m,n,i}}{dx_0^q} \right) = O(\alpha^q), \quad q, n \in 0, 1, 2, \dots, N. \tag{3.7}$$

Substituting equations (3.1)–(3.6) into equations (2.1)–(2.9) and collecting the terms of the like order in  $\varepsilon$  and  $\alpha$ , we obtain the necessary equations to each order of approximation. Then different orders of  $\varepsilon(m)$ ,  $\alpha(n)$  and harmonic ( $i$ ) may be separated, yielding a set of partial differential equations for each index ( $m, n, i$ ). Following these assumptions, analytical solutions for the problem under consideration can then be obtained.

(a)  $\varepsilon^1 \alpha^0$ -order approximation

Upon collecting terms of order  $\varepsilon^1 \alpha^0$ , the governing equations of the continuity equation, irrotational flow condition and Bernoulli equation can be expressed as

$$(f_{1,0x_0} + f'_{1,0y_0}) + (g_{1,0y_0} + g'_{1,0y_0}) + [\sigma_{0,0x_0}(f_{1,0t_1} + f'_{1,0t_0}) + \sigma_{0,0y_0}(g_{1,0t_1} + g'_{1,0t_0})]t = 0, \tag{3.8a}$$

$$\sigma_{0,0}[(f_{1,0x_0 t_1} + f'_{1,0x_0 t_0}) + (g_{1,0y_0 t_1} + g'_{1,0y_0 t_0})] + [\sigma_{0,0x_0}(f_{1,0t_1} + f'_{1,0t_0}) + \sigma_{0,0y_0}(g_{1,0t_1} + g'_{1,0t_0})] + \sigma_{0,0}[\sigma_{0,0x_0}(f_{1,0t_1}^2 + f'_{1,0t_0}^2) + \sigma_{0,0y_0}(g_{1,0t_1}^2 + g'_{1,0t_0}^2)]t = 0, \tag{3.8b}$$

$$\sigma_{0,0}[(f_{1,0y_0 t_1} + f'_{1,0y_0 t_0}) - (g_{1,0x_0 t_1} + g'_{1,0x_0 t_0})] + [\sigma_{0,0y_0}(f_{1,0t_1} + f'_{1,0t_0}) - \sigma_{0,0x_0}(g_{1,0t_1} + g'_{1,0t_0})] + \sigma_{0,0}[\sigma_{0,0y_0}(f_{1,0t_1}^2 + f'_{1,0t_0}^2) - \sigma_{0,0x_0}(g_{1,0t_1}^2 + g'_{1,0t_0}^2)]t = 0, \tag{3.8c}$$

$$\phi_{1,0x_0} + \phi'_{1,0x_0} + \sigma_{0,0x_0}t(\phi_{1,0t_1} + \phi'_{1,0t_0}) + M_{1,0,0} = \sigma_{0,0}(f_{1,0t_1} + f'_{1,0t_0}), \tag{3.8d}$$

$$\phi_{1,0y_0} + \phi'_{1,0y_0} + \sigma_{0,0y_0}t(\phi_{1,0t_1} + \phi'_{1,0t_0}) = \sigma_{0,0}(g_{1,0t_1} + g'_{1,0t_0}) \tag{3.8e}$$

and 
$$\frac{P_{1,0}}{\rho} = -\sigma_{0,0}(\phi_{1,0t_1} + \phi'_{1,0t_0}) - g(g_{1,0} + g'_{1,0}) - gy_0. \tag{3.8f}$$

The condition for zero pressure at the free surface is

$$P_{1,0} = 0 \quad \text{and} \quad y_0 = 0, \tag{3.8g}$$

while the bottom boundary condition is

$$g_{1,0t_1} + g'_{1,0t_0} = 0 \quad \text{and} \quad y = y_0 = -d \tag{3.8h}$$

and time-averaged and stationary mass flux conservation conditions in  $x$ - and  $y$ -direction are

$$\frac{1}{T} \int_0^T \int_{-d}^0 \sigma_{0,0}(g_{1,0t_1} + g'_{1,0t_0}) dy_0 dt = 0 \tag{3.8i}$$

and

$$\frac{1}{T} \int_0^T \int_{-d}^0 \sigma_{0,0}(f_{1,0t_1} + f'_{1,0t_0}) dy_0 dt - \frac{1}{T} \int_0^T \int_{-d_0}^0 \sigma_{0,0}(f_{1,0t_1}^c + f'_{1,0t_0}^c) dy_0 dt = 0. \tag{3.8j}$$

The solutions for equations (3.8a)–(3.8j) can be easily obtained as

$$\left. \begin{aligned} f_{1,0} &= A_{1,0,1}(x_0) \cosh k_{0,0}(y_0 + d) \sin S, \\ g_{1,0} &= B_{1,0,1}(x_0) \sinh k_{0,0}(y_0 + d) \cos S, \\ A_{1,0,1} &= -B_{1,0,1}, \quad f'_{1,0} = g'_{1,0} = \sigma_{0,0a} = \sigma_{0,0b} = \phi'_{1,0} = 0, \\ \phi_{1,0} &= -\frac{\sigma_{0,0}}{k_{0,0}} A_{1,0,1}(x_0) \cosh k_{0,0}(y_0 + d) \sin S, \\ \frac{P_{1,0}}{\rho} &= -gy_0 + gA_{1,0,1}(x_0) \frac{\sinh k_{0,0}y_0}{\cosh k_{0,0}d} \cos S \\ \text{and} \quad \sigma_{0,0}^2 &= gk_{0,0} \tanh k_{0,0}d. \end{aligned} \right\} \tag{3.9}$$

It is obvious that the solutions are not affected by the sloping bottom at this order.

(b)  $\epsilon^1 \alpha^1$ -order approximation

To the next order in  $O(\epsilon^1 \alpha^1)$ , the governing equations are given by

$$\begin{aligned} & [A_{1,0,1x_0} \cosh k_{0,0}(y_0 + d) + A_{1,0,1} k_{0,0x_0}(y_0 + d) \sinh k_{0,0}(y_0 + d) \\ & + A_{1,0,1} k_{0,0} d_{x_0} \sinh k_{0,0}(y_0 + d)] \sin S + \alpha k_{0,1} A_{1,0,1} \cosh k_{0,0}(y_0 + d) \cos S \\ & + \alpha [-A_{1,1,1} k_{0,0} \sin S + B_{1,1,1y_0} \sin S] = 0, \end{aligned} \tag{3.10a}$$

$$\begin{aligned} & -\sigma_{0,0} [A_{1,0,1x_0} \cosh k_{0,0}(y_0 + d) + A_{1,0,1} k_{0,0x_0}(y_0 + d) \sinh k_{0,0}(y_0 + d) \\ & + A_{1,0,1} k_{0,0} d_{x_0} \sinh k_{0,0}(y_0 + d)] \cos S + \alpha \sigma_{0,0} k_{0,1} A_{1,0,1} \cosh k_{0,0}(y_0 + d) \\ & \times \sin S + \alpha \sigma_{0,0} [A_{1,1,1} k_{0,0} \cos S - B_{1,1,1y_0} \cos S] = 0, \end{aligned} \tag{3.10b}$$

$$\begin{aligned} & -\sigma_{0,0} [B_{1,0,1x_0} \sinh k_{0,0}(y_0 + d) + B_{1,0,1} k_{0,0x_0}(y_0 + d) \cosh k_{0,0}(y_0 + d) \\ & + B_{1,0,1} k_{0,0} d_{x_0} \cosh k_{0,0}(y_0 + d)] \sin S + \alpha \sigma_{0,0} k_{0,1} B_{1,0,1} \sinh k_{0,0}(y_0 + d) \\ & \times \cos S + \alpha \sigma_{0,0} [-B_{1,1,1} k_{0,0} \sin S + A_{1,1,1y_0} \sin S] = 0, \end{aligned} \tag{3.10c}$$

$$\begin{aligned} & [\phi_{1,0,1x_0} \sin S + \alpha k_{0,1} \phi_{1,0,1} \cos S - \alpha k_{0,0} \phi_{1,1,1} \sin S + M_{1,1,0}] \\ & = \alpha \sigma_{0,0} A_{1,1,1} \sin S, \end{aligned} \tag{3.10d}$$

$$\alpha\phi_{1,1,1y_0} \cos S = -\alpha\sigma_{0,0}B_{1,1,1} \cos S \tag{3.10e}$$

and  $\alpha \frac{P_{1,1}}{\rho} = -\alpha\sigma_{0,0}\phi_{1,1,1} \sin S - g\alpha B_{1,1,1} \sin S,$  (3.10f)

and the boundary conditions at the free surface and the bottom are

$$P_{1,1} = 0, \quad y_0 = 0 \tag{3.10g}$$

and

$$\sigma_{0,0}\alpha[-B_{1,1,1} \cos S + A_{1,0,1} \cosh k_{0,0}(y_0 + d) \cos S] = 0, \quad y = y_0 = -d. \tag{3.10h}$$

A general solution for  $A_{1,1,1}$  and  $B_{1,1,1}$ , which satisfies both continuity equation and irrotational flow condition, can be assumed as

$$\begin{aligned} \alpha A_{1,1,1} = & [M_{12}(y_0 + d)^2 + M_{11}(y_0 + d) + M_{10}] \cosh k_{0,0}(y_0 + d) \\ & + [N_{11}(y_0 + d) + N_{10}] \sinh k_{0,0}(y_0 + d) \end{aligned} \tag{3.11}$$

and

$$\begin{aligned} \alpha B_{1,1,1} = & [M_{12}(y_0 + d)^2 + M_{11}(y_0 + d) + M_{10}] \sinh k_{0,0}(y_0 + d) \\ & + [N_{11}(y_0 + d) + N_{10}] \cosh k_{0,0}(y_0 + d). \end{aligned} \tag{3.12}$$

Substituting equations (3.11) and (3.12) into equations (3.10a), (3.10b) and (3.10c) and omitting the secular term, the complex constants  $M_{1n}$  and  $N_{1n}$  are found to be

$$\left. \begin{aligned} M_{12} = \frac{1}{2} B_{1,0,1} k_{0,0} x_0, \quad M_{11} = B_{1,0,1} k_{0,0} d x_0, \quad M_{10} = \frac{\alpha B_{1,0,1}}{D^2 \tanh k_{0,0} d}, \quad D = 1 + \frac{2k_{0,0} d}{\sinh 2k_{0,0} d} \\ \text{and} \quad N_{12} = 0, \quad N_{11} = B_{1,0,1} x_0, \quad N_{10} = \alpha A_{1,0,1}, \quad k_{0,1} = M_{1,1,0} = 0. \end{aligned} \right\} \tag{3.13}$$

Further substituting equation (3.13) into equation (3.10e) and using the free surface boundary condition, equation (3.10g), we can obtain

$$B_{1,0,1} = \frac{a}{\sinh k_{0,0} d}, \quad a = \frac{a_0}{\sqrt{k_{0,0} d \operatorname{sech}^2 k_{0,0} d + \tanh k_{0,0} d}} = a_0 K_s, \tag{3.14}$$

where  $a_0$  is the amplitude of the incident waves in deep water and  $a$  is that on the sloping bottom;  $a_0$  and  $a$  are related as follows:

$$a = \frac{a_0}{\sqrt{D \tanh k_0 d}} = a_0 K_s, \tag{3.15}$$

where parameter  $K_s$  is the conventional shoaling coefficient. Based on the solutions derived, let us briefly discuss the effect of bottom slope on the free surface displacement  $y(x_0, y_0 = 0, t)$ . First, the correction to the free surface displacement at  $O(\epsilon^1 \alpha^1)$  is  $90^\circ$  out of phase with respect to the leading order solution ( $\epsilon^1 \alpha^0$ ).

Second, the wave amplitude is enhanced and the phase is modified owing to the effect of the slope. The solutions of  $\varepsilon^1\alpha^1$  are completely determined as

$$\begin{aligned}
 A_{1,1,1} &= B_{1,0,1} \left\{ \left[ \frac{k_{0,0}^2(y_0 + d)^2}{D \sinh 2k_{0,0}d} - k_{0,0}(y_0 + d) + \frac{1}{D^2 \tanh k_{0,0}d} \right] \cosh k_{0,0}(y_0 + d) \right. \\
 &\quad \left. + \left[ \frac{k_{0,0}(y_0 + d)}{D^2 \tanh k_{0,0}d} + \frac{2k_{0,0}(y_0 + d)}{D \sinh 2k_{0,0}d} - 1 \right] \sinh k_{0,0}(y_0 + d) \right\}, \\
 B_{1,1,1} &= B_{1,0,1} \left\{ \left[ \frac{k_{0,0}^2(y_0 + d)^2}{D \sinh 2k_{0,0}d} - k_{0,0}(y_0 + d) + \frac{1}{D^2 \tanh k_{0,0}d} \right] \sinh k_{0,0}(y_0 + d) \right. \\
 &\quad \left. + \left[ \frac{k_{0,0}(y_0 + d)}{D^2 \tanh k_{0,0}d} + \frac{2k_{0,0}(y_0 + d)}{D \sinh 2k_{0,0}d} - 1 \right] \cosh k_{0,0}(y_0 + d) \right\}, \\
 \phi_{1,1,1} &= -\frac{\sigma_{0,0}}{k_{0,0}} B_{1,0,1} \left\{ \left[ \frac{k_{0,0}^2(y_0 + d)^2}{D \sinh 2k_{0,0}d} - k_{0,0}(y_0 + d) \right] \cosh k_{0,0}(y_0 + d) \right. \\
 &\quad \left. + \frac{k_{0,0}(y_0 + d)}{D^2 \tanh k_{0,0}d} \sinh k_{0,0}(y_0 + d) \right\}, \\
 \frac{P_{1,1}}{\rho} &= -[\sigma_{0,0}\phi_{1,1,1} + gB_{1,0,1}] \sin S \\
 \text{and } k_{0,1} &= \sigma_{0,1} = 0.
 \end{aligned} \tag{3.16}$$

The parametric functions for the water particle at any position in Lagrangian coordinates  $(x, y)$  up to the  $\varepsilon^1\alpha^1$  order are given as

$$\frac{(x - x_0)^2}{(B_{1,0,1} \cosh(k_{0,0}(b + d)))^2 + (\alpha A_{1,1,1})^2} + \frac{(y - y_0)^2}{(B_{1,0,1} \sinh(k_{0,0}(b + d)))^2 + (\alpha B_{1,1,1})^2} = 1. \tag{3.17}$$

Figure 2 shows the trajectories up to  $\varepsilon^1\alpha^1$  order of a progressive wave over a sloping bottom; the orbital shape is clearly varying with the depth. The angle  $\beta$  between its main axis and the horizontal axis can also be calculated by coordinate transformation. Neglecting terms of orders higher than  $O(\varepsilon^2\alpha^0)$ , the inclination  $\beta$  can be given by

$$\tan \beta = -\alpha \left[ \frac{k_{0,0}(y_0 + d)}{D^2 \tanh k_{0,0}d} + \frac{2k_{0,0}(y_0 + d)}{D \sinh 2k_{0,0}d} - 1 \right]. \tag{3.18}$$

In equation (3.18),  $\tan \beta$  increases as the water depth  $d$  decreases. It eventually approaches a maximum ( $\tan \beta = \alpha$ ) at bottom  $y_0 = -d$ , where the slope of the main axis coincides with the slope along the direction of a wave ray over the sloping bottom. This implies that a water particle moves along the bottom surface. Figure 2 also shows that the inclination  $\beta$  of a water particle trajectory increases with the decrease in water depth ( $k'_{0,0}d$ ) and bottom slope.

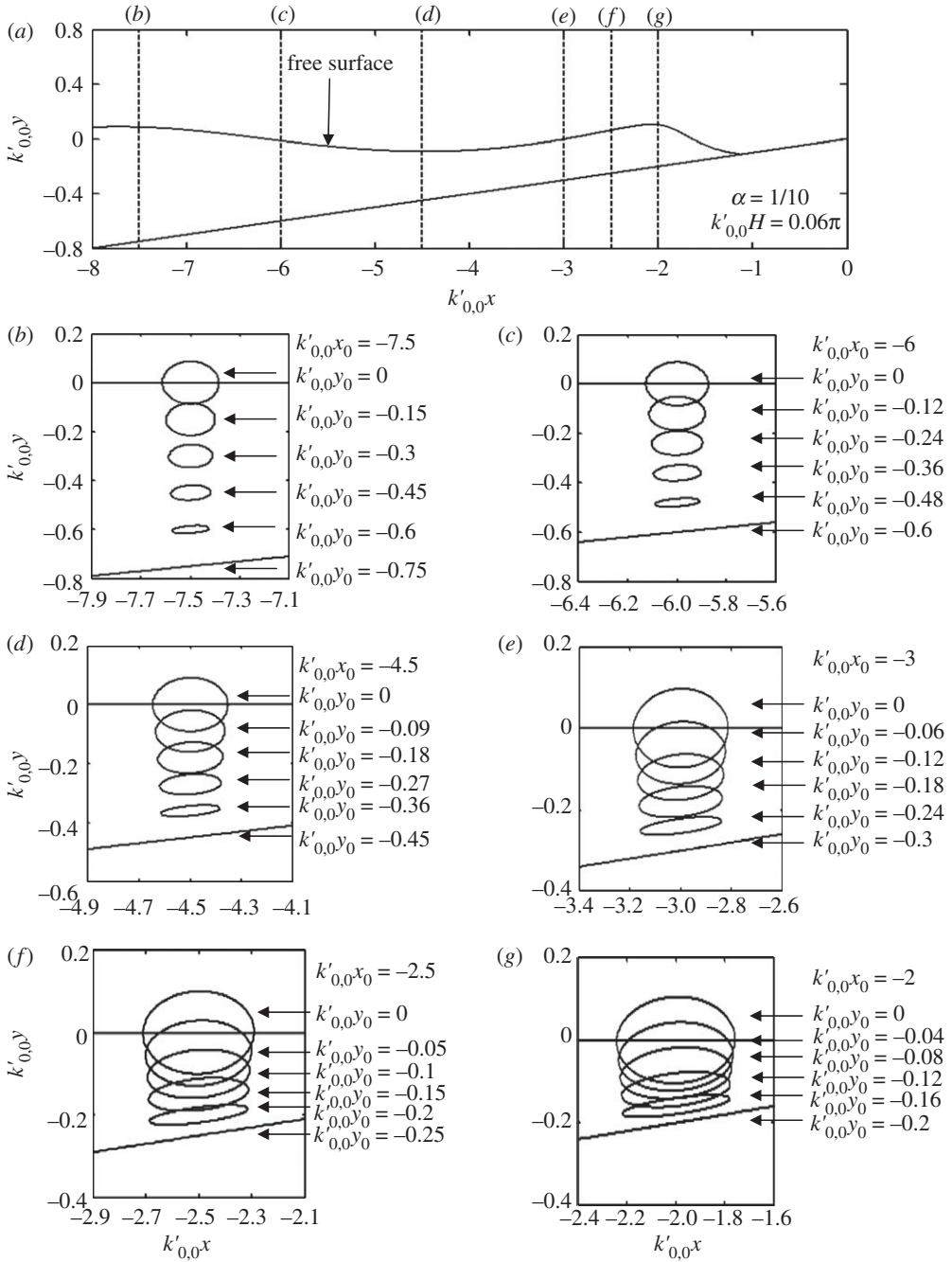


Figure 2. (a-g) The particle trajectories up to  $\varepsilon^1\alpha^1$  order for a progressive wave over a sloping bottom.

Downloaded from https://royalsocietypublishing.org/ on 27 April 2023

(c)  $\varepsilon^2\alpha^0$ -order approximation

In the same manner as  $O(\varepsilon^1\alpha^1)$  is solved, the governing equations in  $O(\varepsilon^2\alpha^0)$  are given by

$$\begin{aligned} & f_{2,0x_0} + f'_{2,0x_0} + g_{2,0y_0} + g'_{2,0y_0} \\ &= \frac{1}{2}A_{1,0,1}^2 k_{0,0}^2 \cosh[2k_{0,0}(y_0 + d)] + \frac{1}{2}A_{1,0,1}^2 k_{0,0}^2 \cos 2S - A_{1,0,1} k_{1,0} \\ &\quad \times \cosh k_{0,0}(y_0 + d) \cos S - [\sigma_{1,0x_0} t f_{1,0t_1} + \sigma_{1,0y_0} g_{1,0t_1}] t, \end{aligned} \tag{3.19a}$$

$$\begin{aligned} & \sigma_{0,0}[f_{2,0x_0} t_1 + f'_{2,0x_0} t_0 + g_{2,0y_0} t_1 + g'_{2,0y_0} t_0] + \sigma_{1,0x_0} f_{1,0t_1} + \sigma_{1,0y_0} g_{1,0t_1} \\ &\quad + \sigma_{1,0}(f_{1,0x_0} t_1 + g_{1,0y_0} t_1) + \sigma_{0,0}(\sigma_{1,0x_0} f_{1,0t_0}^2 + \sigma_{1,0y_0} g_{1,0t_0}^2) t \\ &= -\sigma_{0,0} A_{1,0,1} B_{1,0,1} k_{0,0}^2 \sin 2S - \sigma_{0,0} A_{1,0,1} k_{1,0,1} \cosh k_{0,0}(y_0 + d) \sin S, \end{aligned} \tag{3.19b}$$

$$\begin{aligned} & \sigma_{0,0}(f_{2,0y_0} t_1 + f'_{2,0y_0} t_0 - g_{2,0x_0} t_1 - g'_{2,0x_0} t_0) + \sigma_{1,0y_0} f_{1,0t_1} - \sigma_{1,0x_0} g_{1,0t_1} \\ &\quad + \sigma_{0,0}(\sigma_{1,0y_0} f_{1,0t_1}^2 - \sigma_{1,0x_0} g_{1,0t_0}^2) t \\ &= 2\sigma_{0,0} B_{1,0,1}^2 k_{0,0}^2 \cosh k_{0,0}(y_0 + d) \sinh k_{0,0}(y_0 + d) \\ &\quad + \sigma_{0,0} B_{1,0,1} k_{1,0} \sinh k_{0,0}(y_0 + d) \sin S, \end{aligned} \tag{3.19c}$$

$$\begin{aligned} & \phi_{2,0x_0} + \phi'_{2,0x_0} + \sigma_{1,0x_0} t \phi_{1,0t_1} + M_{2,0,0} = \sigma_{0,0}(f_{2,0t_1} + f'_{2,0t_0} + \sigma_{1,0} f_{1,0t_1}) \\ &\quad - \frac{1}{2} \sigma_{0,0} A_{1,0,1}^2 k_{0,0} [\cosh 2k_{0,0}(y_0 + d) + \cos 2S], \end{aligned} \tag{3.19d}$$

$$\phi_{2,0y_0} + \phi'_{2,0y_0} + \sigma_{1,0y_0} t \phi_{1,0t_1} = \sigma_{0,0}(g_{2,0t_1} + g'_{2,0t_0}) + \sigma_{1,0} g_{1,0t_1}, \tag{3.19e}$$

$$\frac{P_{2,0}}{\rho} = -\sigma_{0,0}(\phi_{2,0t_1} + \phi'_{2,0t_1}) - g(g_{2,0} + g'_{2,0}) + \frac{1}{2}(\sigma_{0,0}^2 f_{1,0t_1}^2 + \sigma_{0,0}^2 g_{1,0t_1}^2), \tag{3.19f}$$

$$\sigma_{0,0}(g_{2,0t_1} + g'_{2,0t_0}) = -\sigma_{1,0} B_{1,0,1} \sinh k_{0,0}(y_0 + d) \sin S = 0, \quad y = y_0 = -d, \tag{3.19g}$$

$$P_{2,0} = 0, \quad y_0 = 0, \tag{3.19h}$$

$$\frac{1}{T} \int_0^T \int_{-d}^0 \sigma_0(g_{2,0t_1} + g'_{2,0t_0}) dy_0 dt = 0 \tag{3.19i}$$

and

$$\begin{aligned} & \frac{1}{T} \int_0^T \int_{-d}^0 \sigma_0(f_{2,0t_1} + f'_{2,0t_0}) dy_0 dt \\ &\quad - \frac{U(\alpha)}{T} \int_0^T \int_{-d_0}^0 \sigma_0(f_{2,0t_1}^c + f_{2,0t_0}^c + f_{2,0t_0}^{\prime c}) dy_0 dt = 0, \quad U(\alpha) \begin{cases} 0, & \alpha \neq 0, \\ 1, & \alpha = 0. \end{cases} \end{aligned} \tag{3.19j}$$

Although laborious, the procedure to obtain the solutions at this order is lengthy, but using straightforward manipulations, the solutions can be given by

$$\left. \begin{aligned}
 f_{2,0} &= -\frac{3}{8} a^2 k_{0,0} \frac{\cosh 2k_{0,0}(y_0 + d)}{\sinh^4 k_{0,0} d} \sin 2S + \frac{1}{4} a^2 k_{0,0} \frac{\sin 2S}{\sinh^2 k_{0,0} d}, \\
 f'_{2,0} &= \frac{1}{2} a^2 k_{0,0} \frac{\cosh 2k_{0,0}(y_0 + d)}{\sinh^2 k_{0,0} d} \sigma_{0,0} t - \frac{gk_{0,0}^2 a^2}{2k_{0,0} d \sigma_{0,0}} t + U(\alpha) \frac{gk_{0,0} k'_{0,0} a_0^2}{2k_{0,0} d \sigma_{0,0}} t, \\
 g_{2,0} &= \frac{3}{8} a^2 k_{0,0} \frac{\sinh 2k_{0,0}(y_0 + d)}{\sinh^4 k_{0,0} d} \cos 2S + \frac{1}{4} a^2 k_{0,0} \frac{\sinh 2k_{0,0}(y_0 + d)}{\sinh^2 k_{0,0} d} \\
 &\quad + \frac{a_0^2 k'_{0,0}}{2 \sinh 2k'_{0,0} d_0} - \frac{a^2 k_{0,0}}{2 \sinh 2k_{0,0} d}, \\
 g'_{2,0} &= \sigma_{1,0} = k_{1,0} = 0, \\
 \phi'_{2,0} &= -\frac{1}{4} a_0^2 \sigma_{0,0}^2 \frac{1}{\sinh^2 k'_{0,0} d_0} t \\
 \text{and } \phi_{2,0} &= \frac{3}{8} a^2 \sigma_{0,0} \frac{\cosh 2k_{0,0}(y_0 + d)}{\sinh^4 k_{0,0} d} \sin 2S - \frac{1}{2} a^2 \sigma_{0,0} \frac{1}{\sinh^2 k_{0,0} d} \sin 2S \\
 &\quad + \int \left[ -\frac{gk_{0,0}^2 a^2}{2k_{0,0} d \sigma_0} + U(\alpha) \frac{gk_{0,0} k'_{0,0} a_0^2}{k_{0,0} d \sigma_0} \right] dx_0.
 \end{aligned} \right\} \tag{3.20a-g}$$

In equation (3.20a-g),  $k'_{0,0}$  is the wavenumber in deep water. The horizontal Lagrangian particle trajectory in the second-order approximation includes a periodic component  $f_{2,0}$ , which is similar to the form of the second-order Lagrangian oscillatory term of constant depth, non-periodic function  $f'_{2,0}$  that increases linearly in time and represents the mass transport and the return flow term. This implies that on average, a fluid particle moves forward and does not form a closed orbit as occurs in the first-order approximation. Differentiating non-periodic function  $f'_{2,0}$  with respect to time, we can obtain the mass transport velocity  $U_L$  of particle as

$$U_L = \frac{1}{2} a^2 \sigma_{0,0} k_{0,0} \frac{\cosh 2k_{0,0}(y_0 + d)}{\sinh^2 k_{0,0} d} - \frac{gk_{0,0}^2 a^2}{2k_{0,0} d \sigma_{0,0}} + U(\alpha) \frac{gk_{0,0} k'_{0,0} a_0^2}{2k_{0,0} d \sigma_{0,0}}. \tag{3.21}$$

The first term in equation (3.21) is the drift velocity over the whole range of depths. It is a second-order correction quantity that has been obtained previously by Longuet-Higgins [37] in the limit of constant water depth. The last two terms in equation (3.21) are for the return flow. This term has not yet been fully discussed besides Chen and co-workers [8,36] and can be used to estimate the return flow for waves progressing over a sloping bottom. In figure 3a, the horizontal mass transport velocity is given for different dimensionless water depths with initial

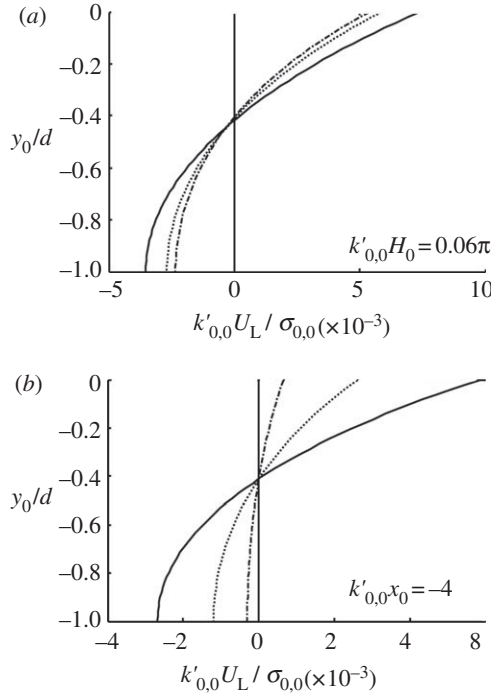


Figure 3. (a) Dimensionless mass transport velocity  $k'_{0,0} U_L / \sigma_{0,0}$  versus dimensionless water depth  $y_0/d$  on three different positions over the slope (solid line,  $k'_{0,0} x_0 = -2$ ; dashed line,  $k'_{0,0} x_0 = -4$ ; dashed-dotted line,  $k'_{0,0} x_0 = -6$ ). (b) Dimensionless mass transport velocity  $k'_{0,0} U_L / \sigma_{0,0}$  versus dimensionless water depth  $y_0/d$  on three different water steepnesses at  $k'_{0,0} x_0 = -4$  (solid line,  $k'_{0,0} H = 0.06\pi$ ; dashed line,  $k'_{0,0} H = 0.04\pi$ ; dashed-dotted line,  $k'_{0,0} H = 0.02\pi$ ).

wave steepness  $k'_{0,0} H_0 = 0.06\pi$  and bottom slope  $\alpha = 1/10$ . The velocity decreases when the dimensionless water depth increases and the mass transport velocity is outward to the sea near the sea bottom. Figure 3b shows the mass transport velocity for different wave steepnesses,  $\alpha = 1/10$  and  $k'_{0,0} x_0 = 1.5$ . For a given dimensionless water depth, the mass transport velocity increases as the wave steepness increases.

The vertical trajectory  $y$  in this order includes a second harmonic component, a Lagrangian mean level that is a function of  $y_0$  and independent of time and a mean sea-level change. This second-order vertical mean level  $g'_{2,0}$  of particles decays with water depth. Equation (3.20d),

$$\frac{1}{4} a^2 k_{0,0} \frac{\sinh 2k_{0,0}(y_0 + d)}{\sinh^2 k_{0,0} d},$$

also confirms that the Lagrangian mean level of gravity waves is higher than the Eulerian mean level. Unlike Longuet-Higgins [38] who used the Euler–Lagrange transformation to derive the above result, the present theory is entirely constructed in the Lagrangian framework. The mean sea-level change was first predicted by Longuet-Higgins & Stewart [39] as the consequence of radiation

stresses. If we consider the case of waves originating from deep-water depth, the wave set-down,

$$\frac{a_0^2 k'_{0,0}}{2 \sinh 2k'_{0,0} d_0} - \frac{a^2 k_{0,0}}{2 \sinh 2k_{0,0} d},$$

is exactly the one that has been obtained by Longuet-Higgins & Stewart.

Figure 4 shows the second-order trajectories of a progressive wave over a sloping bottom. Owing to the second-order mass transport velocity that decreases exponentially with the water depth, the particles do not move in closed orbital motion and each particle advances a larger horizontal movement at the free surface. Near the bottom, the trajectory becomes more like an ellipse since the vertical excursion of the particle is less than its horizontal excursion, in contrast to the trajectories near the mean water level. Even though, the particle in the large amplitude wave has the same features as those noted by Constantin & Varvaruca [40]. Figure 4*f,g* shows that the particle orbit near the surface has an upward convex point or even a secondary loop prior to the wave breaking point. This is due to a secondary wave that will occur in the second-order solution for large wave steepness or highly nonlinear water waves. Hence, the Lagrangian second-order solution presented in this paper is not appropriate for simulating the profile near the wave breaking point owing to the highly nonlinear effects. It remains to extend the present theory to higher order solutions to quantitatively describe the wave-breaking phenomenon.

(d)  $\varepsilon^3 \alpha^0$ -order approximation

Collecting terms of order  $\varepsilon^3 \alpha^0$ , the governing equations and the boundary conditions are

$$\begin{aligned} x_{x_0} y_{y_0} - x_{y_0} y_{x_0} - 1 &= \varepsilon \{f_{1,0x_0}\} + \varepsilon^2 \{ [f_{2,0x_0} + f'_{2,0x_0} + f''_{2,0x_0}] + [f_{1,0x_0} g_{1,0y_0} - f_{1,0y_0} g_{1,0x_0}] \} \\ &+ \varepsilon^3 \{ f_{3,0x_0} + f'_{3,0x_0} + \sigma_{2x_0} t f_{1,0t_1} + g_{3,0y_0} + g'_{3,0y_0} + \sigma_{2y_0} t g_{1,0t_1} + (f_{1,0x_0})(g_{2,0y_0}) \\ &+ (g_{1,0y_0})(f_{2,0x_0} + f'_{2,0x_0}) - (f_{2,0y_0} + f'_{2,0y_0})(g_{1,0x_0}) - (f_{1,0y_0})(g_{2,0x_0} + g'_{2,0x_0}) \}, \end{aligned} \tag{3.22a}$$

$$\begin{aligned} x_{x_0 t} y_{y_0} - x_{x_0 t} y_{y_0} + x_{x_0} y_{y_0 t} - x_{y_0} y_{x_0 t} &= \varepsilon \{ \sigma_0 f_{1,0x_0 t_1} \} + \varepsilon^2 \sigma_0 \{ (f_{2,0x_0 t_1} \\ &+ f'_{2,0x_0 t_1}) + (g_{1,0y_0} \times f_{1,0x_0 t_1}) - (g_{1,0x_0} \times f_{1,0y_0 t_1}) + (g_{2,0y_0 t_1} + g'_{2,0y_0 t_1}) \\ &+ (g_{1,0y_0 t_1} \times f_{1,0x_0}) - (g_{1,0x_0 t_1} \times f_{1,0y_0}) \} \\ &+ \varepsilon^3 \sigma_0 \left\{ \left[ (f_{3,0x_0 t_1} + f'_{3,0x_0 t_1}) + \sigma_{2x_0} t f_{1,0t_1^2} + \frac{\sigma_{2x_0}}{\sigma_0} f_{1,0t_1} + \frac{\sigma_2}{\sigma_0} f_{1,0x_0 t_1} \right] \right. \\ &+ (g_{1,0y_0})(f_{2,0x_0 t_1} + f'_{2,0x_0 t_1}) + (f_{1,0x_0 t_1})(g_{2,0y_0}) \\ &- [(g_{2,0x_0})(f_{1,0y_0 t_1}) + (g_{1,0x_0})(f_{2,0y_0 t_1} + f'_{2,0y_0 t_1})] \\ &+ \left[ (g_{3,0y_0 t_1} + g'_{3,0y_0 t_1}) + \frac{\sigma_{2y_0}}{\sigma_0} (\sigma_0 t g_{1,0t_1^2} + g_{1,0t_1}) + \frac{\sigma_2}{\sigma_0} g_{1,0y_0 t_1} \right] \\ &+ [(g_{1,0y_0 t_1})(f_{2,0x_0} + f'_{2,0x_0}) + (g_{2,0y_0 t_1})(f_{1,0x_0})] - [(g_{2,0x_0 t_1})(f_{1,0y_0}) \\ &\left. + (g_{1,0x_0 t_1})(f_{2,0y_0} + f'_{2,0y_0}) \right] \}, \end{aligned} \tag{3.22b}$$

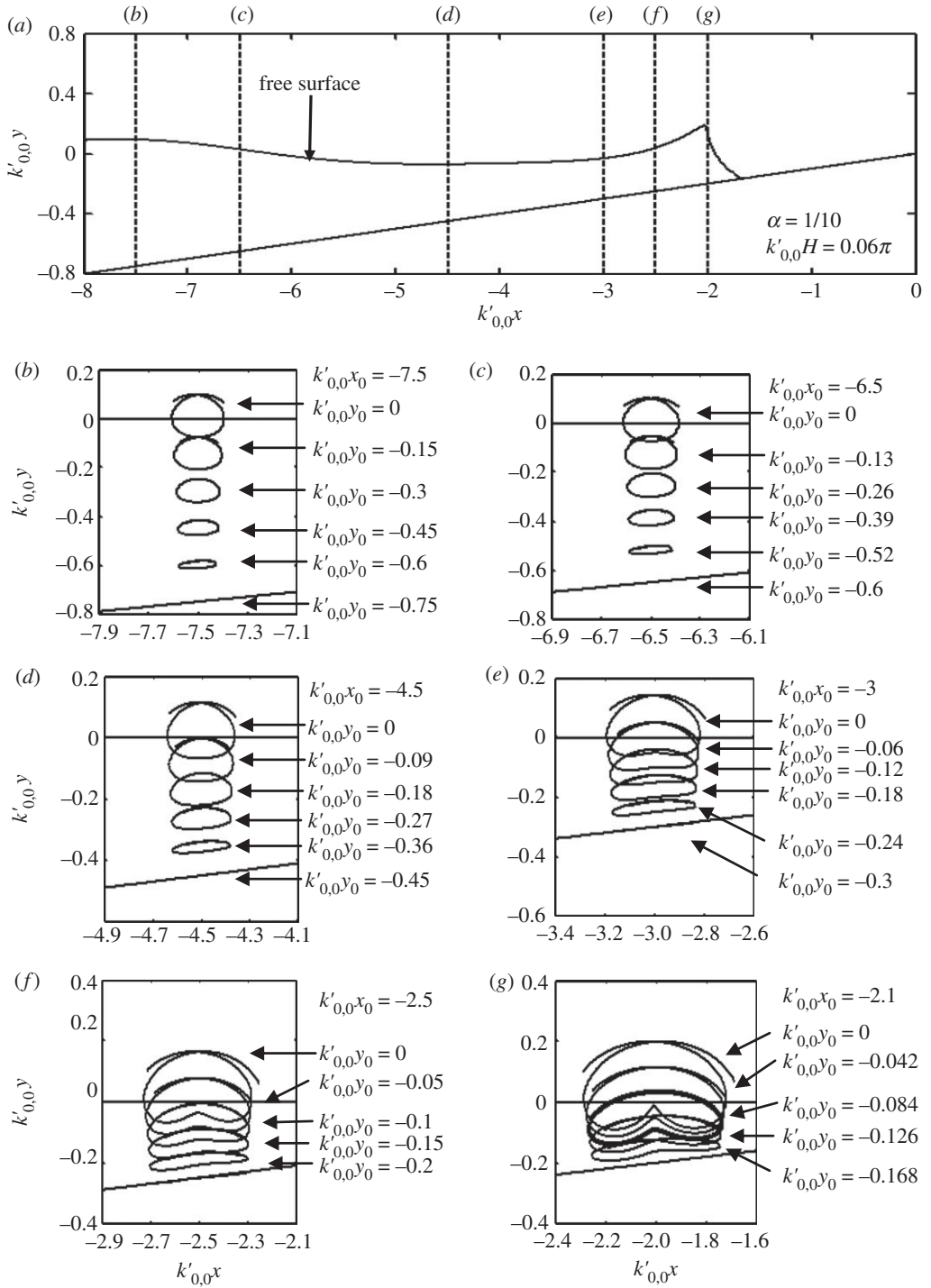


Figure 4. (a–g) The particle trajectories up to  $\varepsilon^2\alpha^0$  order for a progressive wave over a sloping bottom.

$$\begin{aligned}
 x_{y_0 t} x_{x_0} - x_{x_0 t} x_{y_0} + y_{y_0 t} y_{x_0} - y_{x_0 t} y_{y_0} &= \varepsilon \sigma_0 \{-g_{1,0x_0 t_1}\} + \varepsilon^2 \sigma_0 \{(f_{1,0y_0 t_1} \times f_{1,0x_0}) \\
 &- (f_{1,0x_0 t_1} \times f_{1,0y_0}) + (g_{1,0y_0 t_1} \times g_{1,0x_0}) - (g_{1,0x_0 t_1} \times g_{1,0y_0}) - (g_{2,0x_0 t_1})\} \\
 &+ \varepsilon^3 \sigma_0 \left\{ (f_{3,0y_0 t_1} + f'_{3,0y_0 t_0}) + \frac{\sigma_{2y_0}}{\sigma_0} (\sigma_0 t f_{1,0t_1^2} + f_{1,0t_1}) + \frac{\sigma_2}{\sigma_0} f_{1,0y_0 t_1} \right. \\
 &+ (f_{2,0y_0 t_1} + f'_{2,0y_0 t_0})(f_{1,0x_0}) + (f_{1,0y_0 t_1})(f_{2,0x_0} + f'_{2,0x_0}) \\
 &- [(f_{2,0x_0 t_1} + f'_{2,0x_0 t_0})(f_{1,0y_0}) + (f_{1,0x_0 t_1})(f_{1,0y_0} + f'_{1,0y_0})] + (g_{2,0y_0 t_1})(g_{1,0x_0}) \\
 &+ (g_{1,0y_0 t_1})(g_{2,0x_0}) - [g_{2,0x_0 t_1} \times g_{1,0y_0} + g_{1,0x_0 t_1} \times g_{2,0y_0}] \\
 &\left. - \left[ g_{3,0x_0 t_1} + g'_{3,0x_0 t_0} + \frac{\sigma_{2x_0}}{\sigma_0} (\sigma_0 t g_{1,0t_1^2} + g_{1,0t_1}) + \frac{\sigma_2}{\sigma_0} g_{1,0x_0 t_1} \right] \right\}, \tag{3.22c}
 \end{aligned}$$

$$\begin{aligned}
 \phi_{3,0x_0} + \phi'_{3,0x_0} + M_{3,0,0} + \sigma_{2x_0} t \phi_{1,0t_1} + \phi_{1,0x_0} &= \varepsilon^2 \sigma_0 \{f_{1,0t_1} \times f_{1,0x_0} + g_{1,0t_1} \times g_{1,0x_0}\} \\
 &+ \varepsilon^3 \sigma_0 \left\{ \left( f_{3,0t_1} + f'_{3,0t_0} + f''_{3,0t_0} + \frac{\sigma_2}{\sigma_0} f_{1,0t_1} \right) + [(f_{2,0t_1} + f'_{2,0t_0} + f''_{2,0t_0})(f_{1,0x_0}) \right. \\
 &\left. + (f_{1,0t_1})(f_{2,0x_0} + f'_{2,0x_0})] + (g_{2,0t_1})(g_{1,0x_0}) + (g_{1,0t_1})(g_{2,0x_0}) \right\}, \tag{3.22d}
 \end{aligned}$$

$$\begin{aligned}
 \phi_{3,0y_0} + \phi'_{3,0y_0} + \sigma_{2y_0} t \phi_{1,0t_1} &= \sigma_0 \left\{ (f_{2,0t_1} + f'_{2,0t_0} + f''_{2,0t_0})(f_{1,0y_0}) + (f_{1,0t_1})(f_{2,0y_0} + f'_{2,0y_0}) \right. \\
 &\left. + g_{2,0t_1} g_{1,0y_0} + g_{1,0t_1} g_{2,0y_0} + (g_{3,0t_1} + g'_{3,0t_0}) + \frac{\sigma_2}{\sigma_0} g_{1,0t_1} \right\}, \tag{3.22e}
 \end{aligned}$$

$$\begin{aligned}
 \frac{P_{3,0}}{\rho} &= -\sigma_0 (\phi_{3,0t_1} + \phi'_{3,0t_1} + \sigma_2 \phi_{1,0t_1}) - g(g_{3,0} + g'_{3,0}) \\
 &+ \frac{1}{2} \sigma_0^2 [2(f_{1,0t_1})(f_{2,0t_1} + f'_{2,0t_0} + f''_{2,0t_0}) + 2(g_{2,0t_1} \times g_{1,0t_1})], \tag{3.22f}
 \end{aligned}$$

$$P_{3,0} = 0, \quad y_0 = 0, \tag{3.22g}$$

$$g_{3,0t_1} + g'_{3,0t_0} = 0, \quad y = y_0 = -d, \tag{3.22h}$$

$$\frac{1}{T} \int_0^T \int_{-d}^0 \sigma_0 (g_{3,0t_1} + g'_{3,0t_0}) dy_0 dt = 0 \tag{3.22i}$$

and

$$\begin{aligned}
 \frac{1}{T} \int_0^T \int_{-d}^0 [\sigma_0 (f_{3,0t_1} + f'_{3,0t_0} + f''_{3,0t_0}) + \sigma_2 f_{1,0t_1}] dy_0 dt \\
 - \frac{U(\alpha)}{T} \int_0^T \int_{-d}^0 [\sigma_0 (f_{3,0t_1}^c + f'_{3,0t_0}{}^c + f''_{3,0t_0}{}^c) + \sigma_2 f_{1,0t_1}^c] dy_0 dt = 0, \quad U(\alpha) \begin{cases} 0, & \alpha \neq 0, \\ 1, & \alpha = 0. \end{cases} \tag{3.22j}
 \end{aligned}$$

The procedure to obtain the solutions at this order is similar to that of  $O(\varepsilon^2\alpha^0)$ . The solutions can be given by

$$\left. \begin{aligned}
 f_{3,0} &= \left[ -\beta_3 \frac{\cosh 3k_{0,0}(y_0 + d)}{\sinh^3 k_{0,0}d} \right. \\
 &\quad \left. + \frac{1}{6}k_{0,0}(5B_{1,0,1}B_{2,0} - 2B_{1,0,1}C_{2,0}) \cosh k_{0,0}(y_0 + d) \right] \sin 3S \\
 &\quad - \left[ \frac{1}{2}k_{0,0}(5B_{1,0,1}B_{2,0} + 4B_{1,0,1}C_{2,0}) \cosh 3k_{0,0}(y_0 + d) \right. \\
 &\quad \left. + \lambda_3 \frac{\cosh k_{0,0}(y_0 + d)}{\sinh^3 k_{0,0}d} + k_{2,0}B_{1,0,1}(y_0 + d) \sinh k_{0,0}(y_0 + d) \right. \\
 &\quad \left. + \frac{k_{2,0}}{k_{0,0}}B_{1,0,1} \cosh k_{0,0}(y_0 + d) \right] \sin S, \quad f'_{3,0} = 0, \\
 g_{3,0} &= \left[ \beta_3 \frac{\sinh 3k_{0,0}(y_0 + d)}{\sinh^3 k_{0,0}d} - \frac{1}{2}k_{0,0}B_{1,0,1}B_{2,0} \sinh k_{0,0}(y_0 + d) \right] \cos 3S \\
 &\quad + \left[ \frac{1}{2}k_{0,0}(3B_{1,0,1}B_{2,0} + 2B_{1,0,1}C_{2,0}) \sinh 3k_{0,0}(y_0 + d) \right. \\
 &\quad \left. + \lambda_3 \frac{\sinh k_{0,0}(y_0 + d)}{\sinh^3 k_{0,0}d} + k_{2,0}B_{1,0,1}(y_0 + d) \cosh k_{0,0}(y_0 + d) \right. \\
 &\quad \left. + \frac{k_{2,0}}{k_{0,0}}B_{1,0,1} \sinh k_{0,0}(y_0 + d) \right] \cos S, \quad g'_{3,0} = 0, \\
 \phi_{3,0} &= \frac{\sigma_0\beta_3 \cosh 3k_{0,0}(y_0 + d)}{k_{0,0} \sinh^3 k_{0,0}d} \sin 3S + \frac{1}{2}\sigma_0B_{1,0,1}B_{2,0} \cosh 3k_{0,0}(y_0 + d) \sin S \\
 &\quad - \frac{1}{2}\sigma_0B_{1,0,1}(3B_{2,0} - 2C_{2,0}) \cosh k_{0,0}(y_0 + d) \sin 3S \\
 &\quad + \frac{k_{2,0}}{k_{0,0}}\sigma_0B_{1,0,1}(y_0 + d) \sinh k_{0,0}(y_0 + d) \sin S, \\
 \sigma_2 &= -\frac{1}{2}\sigma_0a^2k_{0,0}^2 \frac{\cosh 2k_{0,0}(y_0 + d)}{\sinh^2 k_{0,0}d} + \sigma_{w2} + \sigma_0k_{0,0}(A''_{2,0} + U(\alpha)C''_{2,0}) \\
 \text{and } k_{2,0} &= \frac{k_{0,0}}{D} \left\{ \frac{1}{8}k_{0,0}^2a_0^2(9 \coth^4 k'_{0,0}d_0 - 10 \coth^2 k'_{0,0}d_0 + 9) \right. \\
 &\quad \left. - \frac{1}{8}k_{0,0}^2a^2(9 \coth^4 k_{0,0}d - 10 \coth^2 k_{0,0}d + 9) + A''_{2,0} + U(\alpha)C''_{2,0} \right\},
 \end{aligned} \right\} \tag{3.23}$$

where the coefficients  $\lambda_3, \beta_3, \sigma_{w2}, A_{2,0}, B_{2,0}, C_{2,0}, D_{2,0}$  are

$$\lambda_3 = \frac{-k_{0,0}^2a_0^2a(9 \coth^4 k'_{0,0}d_0 - 10 \coth^2 k'_{0,0}d_0 + 9) \sinh^2 k_{0,0}d}{16},$$

$$\beta_3 = \frac{a^3 k_{0,0}^2 (9 \coth^4 k_{0,0} d - 22 \coth^2 k_{0,0} d + 13)}{64},$$

$$\sigma_{w2} = \frac{k_{0,0}'^2 a_0^2 \sigma_0 (9 \coth^4 k_{0,0}' d_0 - 10 \coth^2 k_{0,0}' d_0 + 9)}{16},$$

$$A_{2,0} = -B_{2,0} = -\frac{3}{8} \frac{B_{1,0,1}^2 k_{0,0}}{\sinh^2 k_{0,0} d}$$

and  $C_{2,0} = D_{2,0} = 2A'_{2,0} = \frac{1}{4} B_{1,0,1}^2 k_{0,0}, A''_{2,0} = \frac{a^2 k_{0,0}^2 g}{2\sigma_0^2 k_{0,0} d}, C''_{2,0} = -\frac{a_0^2 k_{0,0} k_{0,0}' g}{2\sigma_0^2 k_{0,0} d}.$

Figure 5 shows the third-order particle trajectories of a progressive wave over a sloping bottom. Figure 5*f,g* shows that the particle orbit has a downward convex point in the wave trough near the breaking point. Comparing figures 4*g* and 5*g*, it can be seen that the second-order and third-order orbital shapes are different near the wave breaking point.

(e) *The determination of the propagating velocity of the wave surface profile or the wave velocity  $C_w$*

Up to this point, all the properties for the considered waves could be directly found in the Lagrangian framework. The only unsolved property needing to be determined is the wave velocity  $C_w$  since it is varying with the wave surface position and still unknown. The wave velocity  $C_w$  of the considered waves can be obtained as outlined below as shown in figure 6. Consider a surface particle marked with label  $(x_0, y_0 = 0)$  that is located at a point A of the free surface with the horizontal coordinate  $x(x_0, y_0 = 0, t) = x$  and the phase  $\theta = \int^{x_0} k(x'_0) dx'_0 - \sigma t$  at time  $t$ . Along the propagating direction of the free surface, when time  $t + dt, dt \rightarrow 0$ , the point A with the wave velocity  $C_w$  moves a horizontal distance  $C_w dt$  to a new position where an adjacent surface particle marked with label  $(x_0 + dx_0, y_0 = 0)$  travels from time  $t$  to  $t + dt$  to there just to meet it. So, the horizontal coordinate of the new position of the point A at the free surface at time  $t + dt$  is  $x(x_0 + dx_0, y_0 = 0, t + dt) = x + dx$ . From the statement above, two necessary equations for determining the wave velocity  $C_w$  can be written, where the phase  $\theta = \text{constant}$  and  $dt \rightarrow 0, dx_0 \rightarrow 0$ , as follows:

$$\theta = \int^{x_0} k(x'_0) dx'_0 - \sigma t = \int^{x_0 + dx_0} k(x'_0) dx'_0 - \sigma(t + dt) = \text{constant}, y_0 = 0 \quad (3.24)$$

and

$$C_w dt = dx = x(x_0 + dx_0, y_0 = 0, t + dt) - x(x_0, y_0 = 0, t), \quad (3.25)$$

where

$$x(x_0, y_0, t) = x_0 + \sum_{m=1}^{\infty} \sum_{n=0}^{\infty} \epsilon^m \alpha^n \left[ f_{m,n} \left( \int^{x_0} k dx'_0 - \sigma t, y_0 \right) + f'_{m,n}(x_0, y_0, \sigma_0 t) \right]. \quad (3.26)$$

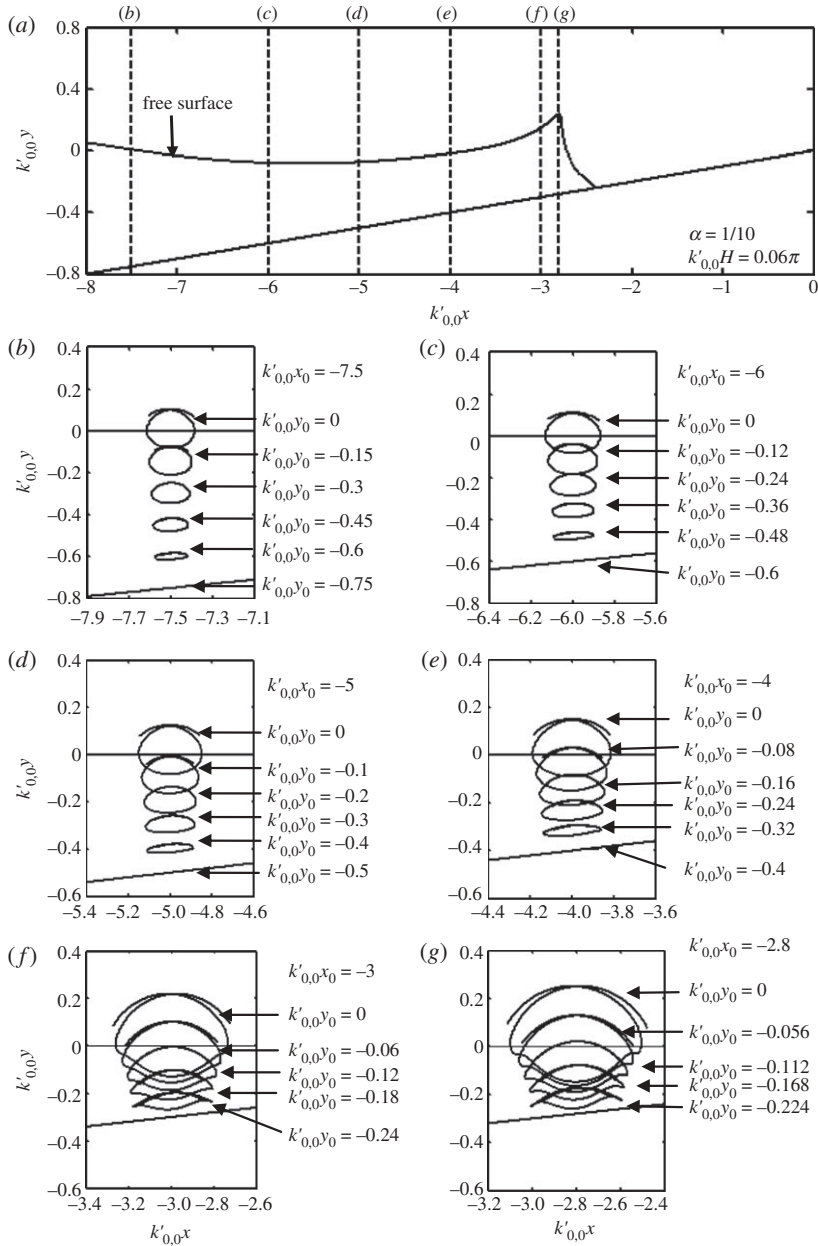


Figure 5. (a–g) The particle trajectories up to  $\varepsilon^3\alpha^0$  order for a progressive wave over a sloping bottom.

The solutions of equations (3.24) and (3.25) are easily to be obtained by using equation (3.26), which are

$$dx_0 = \frac{\sigma}{k} dt \quad \text{and} \quad C_w = \frac{\sigma}{k} + \sum_{m=1}^{\infty} \sum_{n=0}^{\infty} \varepsilon^m \alpha^n \left[ \frac{\sigma f'_{m,n}}{k} \frac{\partial}{\partial x_0} + \frac{f'_{m,n}}{\partial t} \right], \quad y_0 = 0, \quad \frac{\partial^j f_{m,n}}{\partial x_0^j} = O(\alpha^j), \tag{3.27}$$

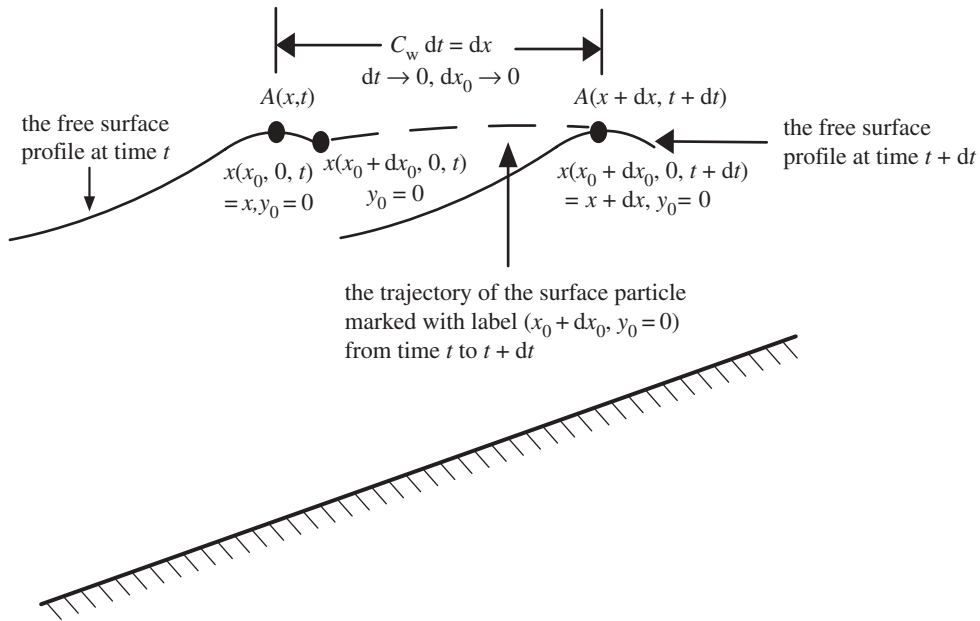


Figure 6. Schematic of the relation between the wave velocity  $C_w$  and the motions of particles at the free surface profile in the waves propagating on the sloping bottom.

respectively. The wave velocity  $C_w$  represented in equation (3.27) is relating to the water depth, the wave steepness, the bottom slope, the wavenumber  $k$ , the frequency  $\sigma$  and the mass transport of particles at the free surface. The result of the wave velocity  $C_w$  in equation (3.27) is consistent with that obtained by Chen *et al.* [27] in the case at uniform water depth as the bottom slope  $\alpha = 0$ . Therefore, the validity of the derivation to the wave velocity in this section is to be conserved and completes the analysis of the considered waves directly in the Lagrangian framework up to  $\varepsilon^3$  order solution.

#### 4. Experimental process

The purpose of the experiments is to quantitatively investigate the characteristics of the water particle behaviour with the progressive gravity waves on a sloping bottom. The experimental processes are stated below.

##### (a) Experimental set-up

To acquire the behaviour of water particle trajectories, a series of experimental measurements were carried out in a glass-walled wave tank,  $20 \times 0.5 \times 0.7$  m, in Tainan Hydraulics Laboratory of National Cheng Kung University, Taiwan. A camera was set up in front of the glass wall about 10–11 m from the wave generator to successively capture the particle motion with the water waves in the tank. Four wave gauges were set up at 2, 3.05, 4.05 and 7 m from the wave generator. The whole experimental frame is schematically shown in figure 7.

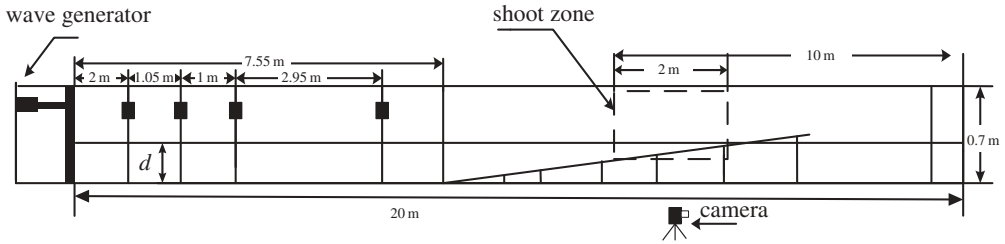


Figure 7. Experimental frame and instrument set-up.

### (b) Experimental procedure

- Monochromatic free surface progressive gravity water waves were generated using a piston-type wave generator.
- Measurements of incident progressive wave elevations were made using a Nijin capacity wave height meter.
- Water particles were simulated with spherical polystyrene beads (PS) of fluorescent red colour with a diameter of about 0.1 cm. The density of primitive PS in a normal state is about  $1.05 \text{ g cm}^{-3}$  heavier than the water. When it is boiled its volume will swell until the density of PS approximately equals water density,  $1.000 \text{ g cm}^{-3}$ .
- Images were captured by a Sony HDR-SR12 digital HD video camera, which has a  $1920 \times 1080$  pixel resolution and 29.97 frames per second maximum framing rate.
- A transparent acrylic-plastic sheet ( $1 \text{ m} \times 45 \text{ cm} \times 2 \text{ mm}$ ), which was placed in the plane of the PS motion position, was calibrated at 1 mm intervals in  $5 \times 5 \text{ mm}$  grids. Its function is a virtual grid in the picture. The trajectory of the PS motion in the water waves could be inferred from the PS motion image data and virtual grid.

### (c) Experimental results

The particle motion experiments were conducted at a constant water depth  $d$  (0.367 m) and various wave periods  $T$  (0.80–2.35 s). The wave height  $H$  was varied over a range 0.0385–0.0672 m. All of the experimental wave conditions are shown in table 1.  $k'_{0,0}x_0$  is the dimensionless initial position of a PS particle. The measured orbital results are shown in figure 8. In figure 8, the two bright horizontal lines are the SWL at both sides of the tank. As in the case of shallow water depth, there is a clearly downward convex shape in the particle orbit, shown in figure 8*a,b*. In figure 8*c*, the PS particle orbit is similar to an ellipse; in figure 8*d,e*, the orbits are non-closed circles.

## 5. Results and discussion

### (a) Verification of the theoretical solution

Verifications of the theoretical solution up to the third order are given below.

(i) In order to verify the theoretical solutions presented above both mathematically and physically, we first prove the asymptotic behaviour for the deep-water limit, as  $d = d_0 \rightarrow \infty$ . In this zone,  $k = k_{0,0} = k'_{0,0}$ ,  $a = a_0$ ,  $D = D_0 = 1$ ,

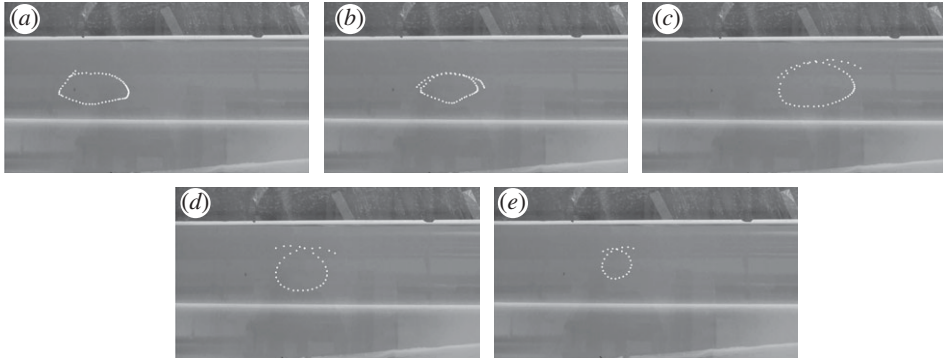


Figure 8. (a–e) The experimental particle trajectories at five wave conditions.

Table 1. Experimental conditions of particle orbit.

no.	$T$ (s)	$H$ (m)	$d$ (m)	$\alpha$	$k'_{0,0}x_0$
a	2.35	0.0385	0.376	1/10	2.3
b	1.74	0.0397	0.376	1/10	3.2
c	2.00	0.0672	0.376	1/10	4
d	1.01	0.0628	0.376	1/10	7
e	0.80	0.0440	0.376	1/10	9

$S = k'_{0,0}x_0 - \sigma t$ . Theoretical solutions in deep water can be easily shown to be

$$\left. \begin{aligned}
 x &= f_{1,0} + f'_{2,0} + f_{3,0} = a_0 e^{k'_{0,0}y_0} \sin S + a_0^2 k'_{0,0} e^{2k'_{0,0}y_0} \sigma_0 t \\
 &\quad - \left[ 2a_0^3 k_{0,0}^2 e^{3k'_{0,0}y_0} - \frac{1}{2} a_0^3 k_{0,0}'^2 e^{k'_{0,0}y_0} \right] \sin S, \\
 y &= g_{1,0} + g_{3,0} = a_0 e^{k'_{0,0}y_0} \cos S + \frac{1}{2} a_0^2 k'_{0,0} e^{2k'_{0,0}y_0} \\
 &\quad + \left[ a_0^3 k_{0,0}^2 e^{3k'_{0,0}y_0} - \frac{1}{2} a_0^3 k_{0,0}'^2 e^{k'_{0,0}y_0} \right] \cos S, \\
 \phi &= \phi_{1,0} = -\frac{\sigma_{0,0}}{k_0} a_0 e^{k'_{0,0}y_0} \sin S, \\
 \sigma_{0,0}^2 &= gk'_{0,0}, \\
 \sigma_{2,0} &= \sigma_0 a_0^2 k_{0,0}'^2 \left( -e^{2k'_{0,0}y_0} + \frac{1}{2} \right)
 \end{aligned} \right\} \tag{5.1}$$

and  $\sigma = \sigma_{0,0} + \sigma_{2,0}$ ,

which are the same as those given by Chen *et al.* [27] in deep water and hence the theory is verified. Apparently, the water particle trajectory in deep water is symmetric and the present deep water solution does not encompass the bottom effect. Constantin and co-workers [41–43] show the symmetry property holds even for waves of large amplitude in the presence of underlying vorticity.

(ii) Constant horizontal depth, viz.  $d = d_c$  and  $\alpha = 0$ . This case describes finite amplitude waves over a constant depth. Since in this case

$$k_{0,0} = k_{0,0c}; a = a_c; S = k_{0,0c}x_0 - \sigma t,$$

for the case of  $\alpha = 0$  the theoretical solution becomes

$$\begin{aligned} x = f_{1,0} + f_{2,0} + f'_{2,0} + f_{3,0} &= -a_c \frac{\cosh k_{0,0c}(y_0 + d_c)}{\sinh k_{0,0c}d_c} \sin S \\ &\quad - \frac{3}{8} a_c^2 k_{0,0c} \frac{\cosh 2k_{0,0c}(y_0 + d_c)}{\sinh^4 k_{0,0c}d_c} \sin 2S + \frac{1}{4} a_c^2 k_{0,0c} \frac{\sin 2S}{\sinh^2 k_{0,0c}d_c} \\ &\quad + \frac{1}{2} a_c^2 k_{0,0c} \frac{\cosh 2k_{0,0c}(y_0 + d_c)}{\sinh^2 k_{0,0c}d_c} \sigma_{0,0} t + \left[ -\beta_{3c} \frac{\cosh 3k_{0,0c}(y_0 + d_c)}{\sinh^3 k_{0,0c}d_c} \right. \\ &\quad \left. + \frac{1}{6} k_{0,0c} (5B_{1,0,1c} B_{2,0c} - 2B_{1,0,1c} C_{2,0c}) \cosh k_{0,0c}(y_0 + d_c) \right] \sin 3S \\ &\quad - \left[ \frac{1}{2} k_{0,0c} (5B_{1,0,1c} B_{2,0c} + 4B_{1,0,1c} C_{2,0c}) \cosh 3k_{0,0c}(y_0 + d_c) \right. \\ &\quad \left. + \frac{\lambda_{3c} \cosh k_{0,0c}(y_0 + d_c)}{\sinh^3 k_{0,0c}d_c} \right] \sin S, \\ y = g_{1,0} + g_{2,0} + g_{3,0} &= a_c \frac{\sinh k_{0,0c}(y_0 + d_c)}{\sinh k_{0,0c}d_c} \cos S \\ &\quad + \frac{3}{8} a_c^2 k_{0,0c} \frac{\sinh 2k_{0,0c}(y_0 + d_c)}{\sinh^4 k_{0,0c}d_c} \cos 2S + \frac{1}{4} a_c^2 k_{0,0c} \frac{\sinh 2k_{0,0c}(y_0 + d_c)}{\sinh^2 k_{0,0c}d_c} \\ &\quad + \left[ \beta_{3c} \frac{\sinh 3k_{0,0c}(y_0 + d_c)}{\sinh^3 k_{0,0c}d_c} - \frac{1}{2} k_{0,0c} B_{1,0,1c} B_{2,0c} \sinh k_{0,0c}(y_0 + d_c) \right] \cos 3S \\ &\quad + \left[ \frac{1}{2} k_{0,0c} (3B_{1,0,1c} B_{2,0c} + 2B_{1,0,1c} C_{2,0c}) \sinh 3k_{0,0c}(y_0 + d_c) \right. \\ &\quad \left. + \lambda_{3c} \frac{\sinh k_{0,0c}(y_0 + d_c)}{\sinh^3 k_{0,0c}d_c} + k_{2,0c} B_{1,0,1c}(y_0 + d_c) \cosh k_{0,0c}(y_0 + d_c) \right] \cos S, \\ \phi = \phi_{1,0} + \phi_{2,0} + \phi'_{2,0} + \phi_{3,0} &= \frac{a_c \sigma_{0,0} \cosh k_{0,0c}(y_0 + d_c)}{k_{0,0c} \sinh k_{0,0c}d_c} \sin S \\ &\quad + \frac{3}{8} a_c^2 \sigma_{0,0} \frac{\cosh 2k_{0,0c}(y_0 + d_c)}{\sinh^4 k_{0,0c}d_c} \sin 2S - \frac{1}{2} a_c^2 \sigma_{0,0} \frac{1}{\sinh^2 k_{0,0c}d_c} \sin 2S \\ &\quad - \frac{1}{4} a_c^2 \sigma_{0,0}^2 \frac{1}{\sinh^2 k_{0,0c}d_c} t + \frac{\sigma_0}{k_{0,0c}} \beta_{3c} \frac{\cosh 3k_{0,0c}(y_0 + d_c)}{\sinh^3 k_{0,0c}d_c} \sin 3S \\ &\quad + \frac{1}{2} \sigma_0 B_{1,0,1c} B_{2,0c} \cosh 3k_{0,0c}(y_0 + d_c) \sin S - \frac{1}{2} \sigma_0 B_{1,0,1c} (3B_{2,0c} - 2C_{2,0c}) \\ &\quad \times \cosh k_{0,0c}(y_0 + d_c) \sin 3S, \sigma_{0,0}^2 = gk_{0,0c} \tanh k_{0,0c}d_c, \\ \sigma_{w2c} &= \frac{1}{16} k_{0,0c}^2 a_c^2 \sigma_0 (9 \coth^4 k_{0,0c}d_c - 10 \coth^2 k_{0,0c}d_c + 9) \\ \text{and } \sigma_2 &= -\frac{1}{2} \sigma_0 B_{1,0,1c}^c k_{0,0c}^2 \cosh 2k_{0,0c}(y_0 + d_c) + \sigma_{w2c}, \end{aligned} \tag{5.2}$$

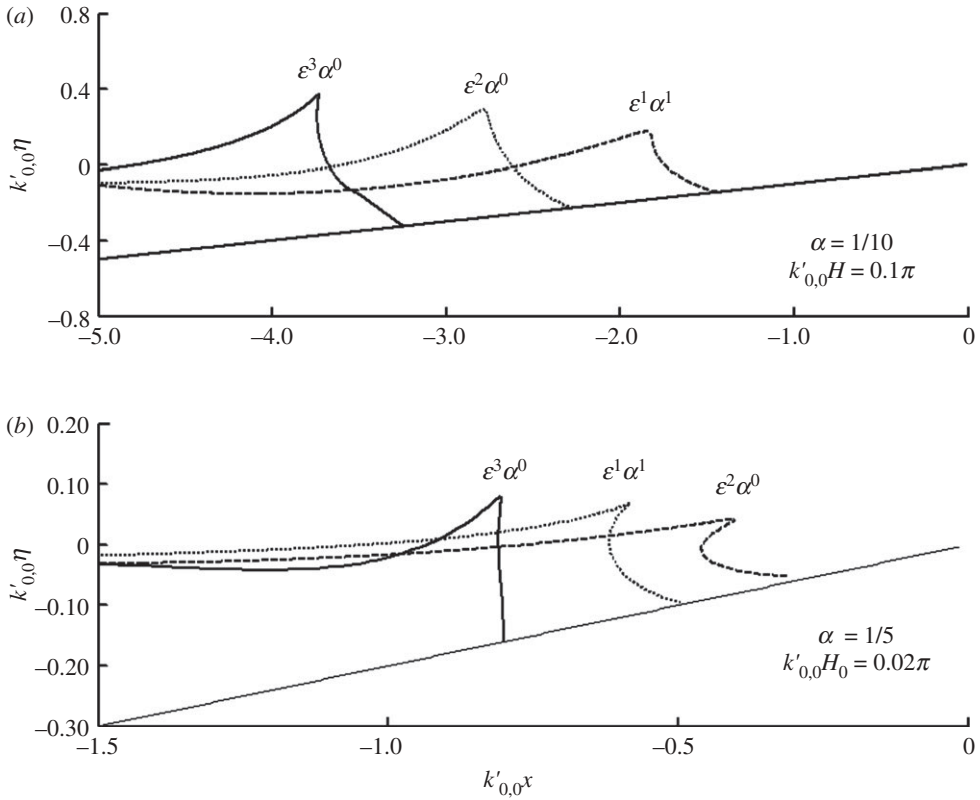


Figure 9. (a, b) Successive wave profiles prior to breaking plotted by linear (up to the order of  $\epsilon^1\alpha^1$ ) and nonlinear solutions (up to the order of  $\epsilon^2\alpha^0$  and up to the order of  $\epsilon^3\alpha^0$ ) under varying wave conditions and bottom slopes. (Solid line, third-order solution; dotted line, second-order solution; dashed line, linear solution.)

where the coefficients  $\beta_{3c}$ ,  $\lambda_{3c}$ ,  $B_{2,0c}$ ,  $C_{2,0c}$  and  $B_{1,0,1}^c$  are

$$\beta_{3c} = \frac{1}{64} a_c^3 k_{0,0c}^2 (9 \coth^4 k_{0,0c} d_c - 22 \coth^2 k_{0,0c} d_c + 13),$$

$$\lambda_{3c} = -\frac{1}{16} k_{0,0c}^3 a_c^2 (9 \coth^4 k_{0,0c} d_c - 10 \coth^2 k_{0,0c} d_c + 9) \sinh^2 k_{0,0c} d_c,$$

$$B_{2,0c} = \frac{3}{8} B_{1,0,1c}^2 k_{0,0c} \frac{1}{\sinh^2 k_{0,0c} d_c},$$

$$C_{2,0c} = \frac{1}{4} B_{1,0,1c}^2 k_{0,0c}$$

and 
$$B_{1,0,1}^c = \frac{a_c}{\sinh k_{0,0c} d_c}.$$

The present theory is reduced to a nonlinear wave over water of constant depth, as was previously obtained by Chen *et al.* [27]. Thus, the present theory is verified.

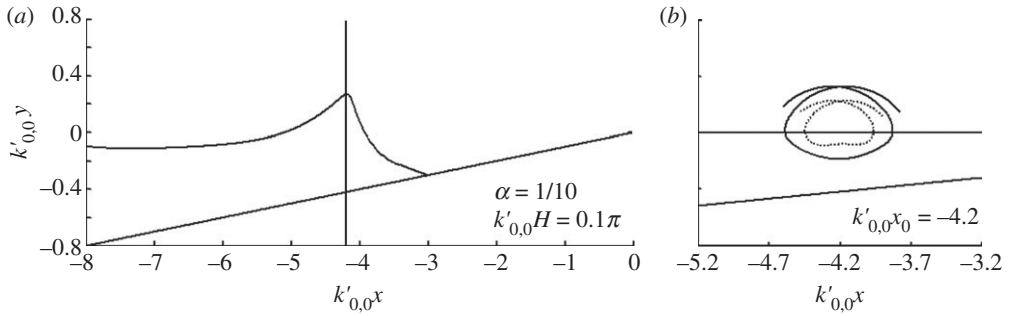


Figure 10. (a, b) The particle trajectories near the wave-breaking point for a spilling wave. (Solid line, up to  $\epsilon^3\alpha^0$  order; dashed line, up to  $\epsilon^2\alpha^0$  order.)

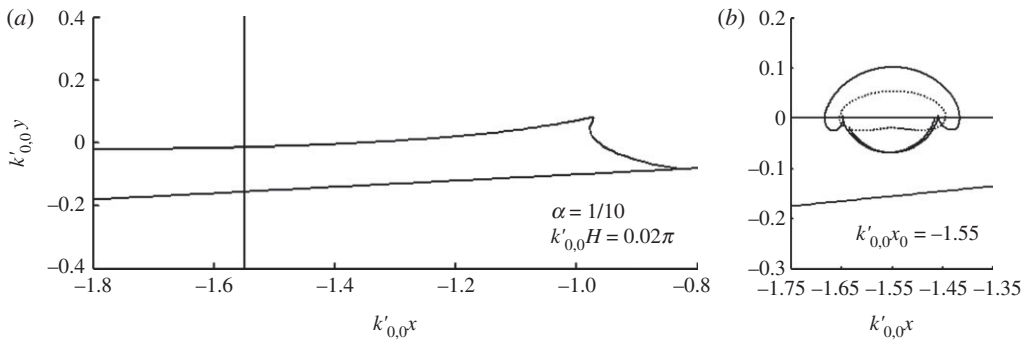


Figure 11. (a, b) The particle trajectories near the wave-breaking point for a plunging wave. (Solid line, up to  $\epsilon^3\alpha^0$  order; dashed line, up to  $\epsilon^2\alpha^0$  order.)

(b) Wave transformations

As the height of a wave reaches its upper limit, the crest is fully developed as a summit that can be calculated as the spatial surface profile by a system of Lagrangian coordinates. In this approach, the new displacement components of water particles  $x$  and  $y$  to the third-order approximation have been obtained as follows:

$$x(x_0, y_0, t) = x_0 + \epsilon^1\alpha^0 f_{1,0} + \epsilon^1\alpha^1 f_{1,1} + \epsilon^2\alpha^0 (f_{2,0} + f'_{2,0}) + \epsilon^3\alpha^0 f_{3,0} \tag{5.3}$$

and

$$y(x_0, y_0, t) = y_0 + \epsilon^1\alpha^0 g_{1,0} + \epsilon^1\alpha^1 g_{1,1} + \epsilon^2\alpha^0 g_{2,0} + \epsilon^3\alpha^0 g_{3,0}. \tag{5.4}$$

The surface wave profiles near the wave breaking point can be evaluated and the results are illustrated in figure 9. The linear (up to the order  $\epsilon^1\alpha^1$ ) and nonlinear solutions (up to the orders  $\epsilon^2\alpha^0$  and  $\epsilon^3\alpha^0$ ) are implemented for comparison. This figure shows the surface wave profiles prior to breaking on different wave steepness and wave phase for bottom slopes of  $\alpha = 1/5$  and  $1/10$ , respectively, based on the wave breaking criterion of  $u/C_w = 1$ . It is found that the third-order theory is consistent with the classification of wave breakers proposed by Galvin [44]. This confirms that the breaker type depends on the bottom slopes. In general, the third-order wave profiles are higher than the second-order and linear solutions

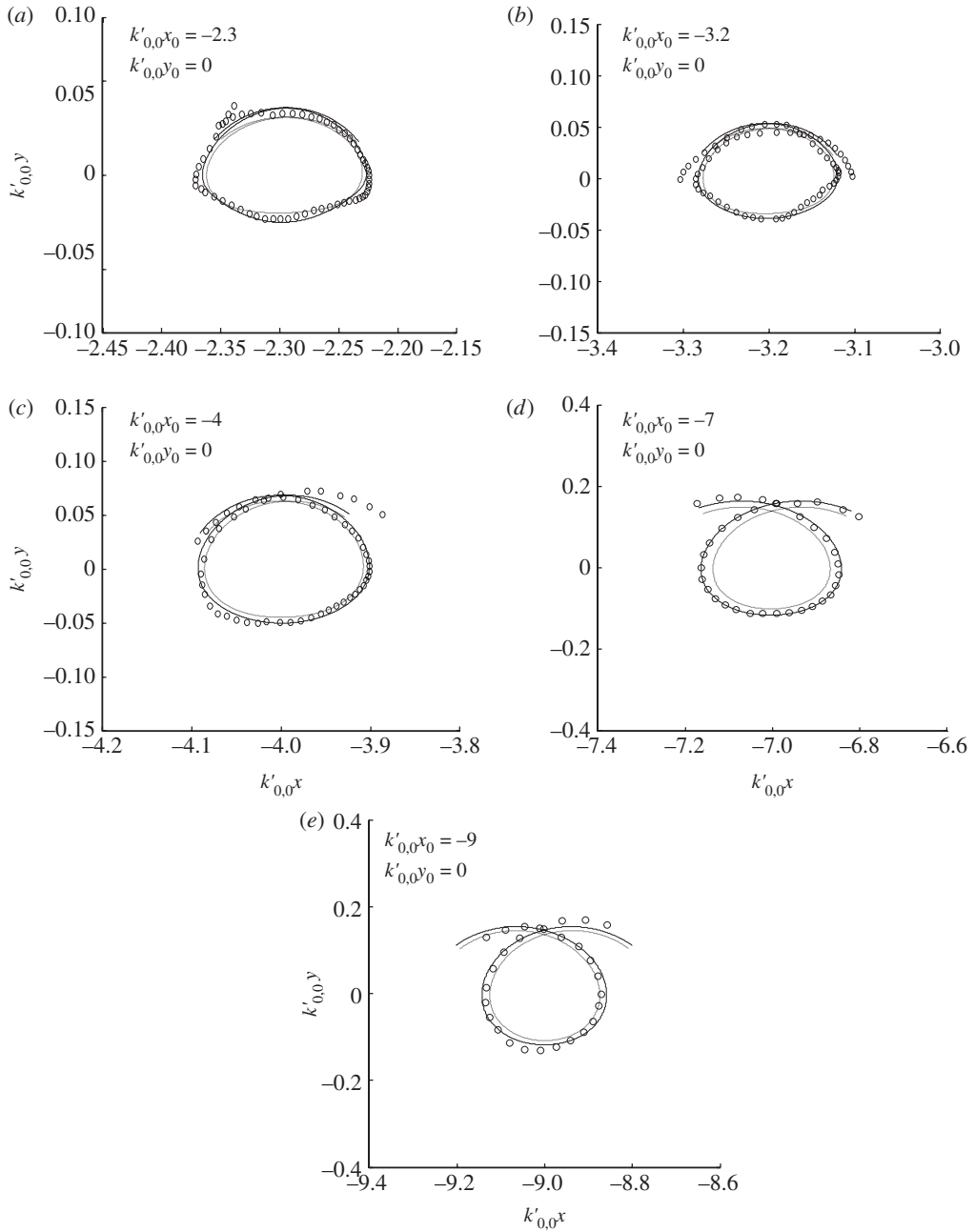


Figure 12. (a–e) Comparisons between the orbits of water particles obtained by the third-order solution, second-order solution and those from the experimental measurements of the PS motions on sloping bottom (circle, experiment; solid line, the third-order solution; dashed line, the second-order solution). (The wave conditions are listed in table 1.)

for any wave steepness and bottom slope. Moreover, the breaking point predicted by the third-order solution occurs earlier than that by the second-order and linear solutions.

### (c) Particle orbits

The new Lagrangian solution for water particle displacement developed in this study can be employed to demonstrate the validity for water particle motion. The parametric functions for the water particle at any position in Lagrangian coordinates  $(x, y)$  are given in equations (5.3) and (5.4). Figures 10 and 11 show the variation of particle trajectories under a spilling and plunging breaker. Owing to the second-order mass transport velocity which decreases exponentially with the water depth, the particles do not move in a closed orbital motion and each particle advances a larger horizontal movement at the free surface. Near the bottom, the trajectory becomes more like an ellipse since the vertical excursion of the particle is less than its horizontal excursion, in contrast with the trajectories near the mean water level. In the same deep water steepness, the second-order orbital motion is smaller than the third-order orbital motion. Figure 12 shows good agreement between the experimental data and the third-order asymptotic solution of the particle trajectories at the free surface.

## 6. Conclusions

This paper provides a new third-order Lagrangian asymptotic solution for surface waves propagating over a uniform sloping beach. The solution, developed in explicit form, includes parametric functions for water particle motion and the wave velocity in Lagrangian description. These explicit expressions enable the description of wave shoaling in the direction of wave propagation from deep to shallow water. The solution also provides information for the process of successive deformation of a wave profile and water particle trajectory. The solution to the nonlinear boundary-value problem is presented after including a mean return current which is needed to maintain zero mass flux in a bounded domain. Also, the Lagrangian mean level differing from the Eulerian mean level is explicitly obtained via a new third-order solution. Furthermore, to check the validity of the nonlinear analytical solution, it is shown analytically that, in the limit of deep water or constant depth, the nonlinear solution reduces to the known Lagrangian third-order solution of progressive waves. A series of experiments measuring the Lagrangian properties of nonlinear water waves propagating over a sloping bottom were conducted in a wave tank. Good agreement has been obtained on comparing the measured trajectories with the theoretical trajectories predicted by the proposed third-order Lagrangian solution.

Dr K. S. Hwang is appreciated for his laboratory assistance. The work was supported by the Research Grant Council of the National Science Center, Taiwan, through project no. NSC99-2923-E-110-001-MY3 and no. NSC99-2221-E-110 -087-MY3.

## References

- 1 Segur, H. 2007 Waves in shallow water, with emphasis on the tsunami of 2004. In *Tsunami and nonlinear waves*, pp. 3–29. Berlin, Germany: Springer.

- 2 Constantin, A. & Johnson, R. S. 2008 Propagation of very long water waves, with vorticity, over variable depth, with applications to tsunamis. *Fluid Dyn. Res.* **40**, 175–211. (doi:10.1016/j.fluidyn.2007.06.004)
- 3 Biesel, F. 1952 Study of wave propagation in water of gradually varying depth. Gravity waves. Circular **521**, pp. 243–253, US National Bureau of Standards.
- 4 Chen, Y.-Y. & Tang, L. W. 1992 Progressive surface waves on gentle sloping bottom. In *Proc. 14th Ocean Engineering Conf. in Taiwan*, pp. 1–22. Taiwan: Taiwan Society of Ocean Engineering. [In Chinese.]
- 5 Carrier, G. F. & Greenspan, H. P. 1958 Water waves of finite amplitude on a sloping beach. *J. Fluid Mech.* **4**, 97–109. (doi:10.1017/S0022112058000331)
- 6 Chu, V. H. & Mei, C. C. 1970 On slowly-varying Stokes waves. *J. Fluid Mech.* **41**, 873–887. (doi:10.1017/S0022112070000988)
- 7 Liu, P. L. F. & Dingemans, M. W. 1989 Derivation of the third-order evolution equations for weakly nonlinear water waves propagating over uneven bottoms. *Wave Motion* **11**, 41–64. (doi:10.1016/0165-2125(89)90012-7)
- 8 Chen, Y.-Y., Hsu, H.-C., Chen, G.-Y. & Hwung, H.-H. 2006 Theoretical analysis of surface waves shoaling and breaking on a sloping bottom. II. Nonlinear waves. *Wave Motion* **43**, 339–356. (doi:10.1016/j.wavemoti.2006.01.002)
- 9 Chen, Y.-Y. & Hsu, H.-C. 2009 A third-order asymptotic solution of nonlinear standing water waves in Lagrangian coordinates. *Chin. Phys. B* **18**, 861–871. (doi:10.1088/1674-1056/18/3/004)
- 10 Naciri, M. & Mei, C. C. 1993 Evolution of short gravity waves on long gravity waves. *Phys. Fluids A* **5**, 1869–1878. (doi:10.1063/1.858812)
- 11 Ng, C. O. 2004 Mass transport in a layer of power-law fluid forced by periodic surface pressure. *Wave Motion* **39**, 241–259. (doi:10.1016/j.wavemoti.2003.10.002)
- 12 Ng, C. O. 2004 Mass transport and set-ups due to partial standing surface waves in a two layer viscous system. *J. Fluid Mech.* **520**, 297–325. (doi:10.1017/S0022112004001624)
- 13 Ng, C. O. 2004 Mass transport in gravity waves revisited. *J. Geophys. Res. Oceans* **109**, C04012. (doi:10.1029/2003JC002121)
- 14 Chen, Y.-Y., Hwung, H.-H. & Hsu, H.-C. 2005 Theoretical analysis of surface waves propagation on sloping bottoms. I. *Wave Motion* **42**, 335–351. (doi:10.1016/j.wavemoti.2005.04.004)
- 15 Zhang, X. & Ng, C.-O. 2006 On the oscillatory and mean motions due to waves in thin viscoelastic layer. *Wave Motion* **43**, 387–405. (doi:10.1016/j.wavemoti.2006.02.003)
- 16 Buldakov, E. V., Taylor, P. H. & Taylor, R. E. 2006 New asymptotic description of nonlinear water waves in Lagrangian coordinates. *J. Fluid Mech.* **562**, 431–444. (doi:10.1017/S0022112006001443)
- 17 Ng, C. O. & Zhang, X. Y. 2007 Mass transport in water waves over a thin layer of soft viscoelastic mud. *J. Fluid Mech.* **573**, 105–130. (doi:10.1017/S0022112006003508)
- 18 Gerstner, F. J. 1802 Theorie de wellen. *Abh. d. K. bohm. Ges. Wiss.* **32**, 412–440. [Reprinted in *Ann. Physik.*]
- 19 Miche, A. 1944 Mouvements ondulatoires de la mer en profondeur constante ou décroissante. *Annal. Ponts Chaussees* **114**, 25–78, 131–164, 270–292, 369–406.
- 20 Pierson, W. J. 1962 Perturbation analysis of the Navier-Stokes equations in Lagrangian form with selected linear solution. *J. Geophys. Res.* **67**, 3151–3160. (doi:10.1029/JZ067i008p03151)
- 21 Constantin, A. 2006 The trajectories of particles in Stokes waves. *Invent. Math.* **166**, 523–535. (doi:10.1007/s00222-006-0002-5)
- 22 Constantin, A. & Escher, J. 2007 Particle trajectories in solitary water waves. *Bull. Am. Math. Soc.* **44**, 423–431. (doi:10.1090/S0273-0979-07-01159-7)
- 23 Constantin, A. & Strauss, W. 2010 Pressure beneath a Stokes wave. *Commun. Pure Appl. Math.* **53**, 533–557. (doi:10.1002/cpa.20299)
- 24 Constantin, A. & Escher, J. 2011 Analyticity of periodic traveling freesurface water waves with vorticity. *Ann. Math.* **173**, 559–568. (doi:10.4007/annals.2011.173.1.12)
- 25 Ehrnström, M. & Wahlen, E. 2008 On the fluid motion in standing waves. *J. Nonlinear Math. Phys.* **15**, 74–86. (doi:10.2991/jnmp.2008.15.s2.6)
- 26 Hsu, H.-C., Chen, Y.-Y. & Wang, C.-F. 2010 Perturbation analysis of the short-crested waves in Lagrangian coordinates. *Nonlinear Anal. Ser. B: Real World Appl.* **11**, 1522–1536. (doi:10.1016/j.nonrwa.2009.03.014)

- 27 Chen, Y.-Y., Hsu, H.-C. & Chen, G.-Y. 2010 Lagrangian experiment and solution for irrotational finite-amplitude progressive gravity waves at uniform depth. *Fluid Dyn. Res.* **42**, 045511. (doi:10.1088/0169-5983/42/4/045511)
- 28 Sanderson, B. 1985 A Lagrangian solution for internal waves. *J. Fluid Mech.* **152**, 191–202. (doi:10.1017/S0022112085000647)
- 29 Constantin, A. 2001 Edge waves along a sloping beach. *J. Phys. A* **34**, 9723–9731. (doi:10.1088/0305-4470/34/45/311)
- 30 Chen, Y.-Y. & Huang, C.-Y. 2000 Surface-waves propagation on a gentle bottom in Lagrangian form. In *Proc. 22nd Conf. on Ocean Engineering in Taiwan*, pp. 79–88. Taiwan: Taiwan Society of Ocean Engineering. [In Chinese.]
- 31 Kapinski, J. 2006 On modeling of long waves in the Lagrangian and Eulerian descriptions. *Coastal Eng.* **53**, 759–765. (doi:10.1016/j.coastaleng.2006.03.009)
- 32 Chen, Y.-Y. 1994 Perturbation analysis of the irrotational progressive gravity waves in fluid of any uniform depth in Lagrangian form. In *Proc. 16th Ocean Engineering Conf. in Taiwan*, pp. A1–A29. Taiwan: Taiwan Society of Ocean Engineering. [In Chinese.]
- 33 Lamb, H. 1932 *Hydrodynamics*, 6th edn. Cambridge, UK: Cambridge University Press.
- 34 Yakubovich, E. I. & Zenkovich, D. A. 2001 Matrix approach to Lagrangian fluid dynamics. *J. Fluid Mech.* **443**, 167–196. (doi:10.1017/S0022112001005195)
- 35 Chen, Y.-Y. 2003 Nonlinear analysis for surface waves propagation on non-steep sloping bottom. I. Systematical perturbation expansion model. In *Proc. 25th Conf. on Ocean Engineering in Taiwan*, pp. 39–48. Taiwan: Taiwan Society of Ocean Engineering. [In Chinese.]
- 36 Chen, Y.-Y. 2003 Nonlinear analysis for surface waves propagation on non-steep sloping bottom. II. Analytical solution up to order and verification. In *Proc. 25th Conf. on Ocean Engineering in Taiwan*, pp. 49–58. Taiwan: Taiwan Society of Ocean Engineering. [In Chinese.]
- 37 Longuet-Higgins, M. S. 1953 Mass transport in water waves. *Phil. Trans. R. Soc. Lond. A* **245**, 535–581. (doi:10.1098/rsta.1953.0006)
- 38 Longuet-Higgins, M. S. 1986 Eulerian and Lagrangian aspects of surface waves. *J. Fluid Mech.* **173**, 683–707. (doi:10.1017/S0022112086001325)
- 39 Longuet-Higgins, M. S. & Stewart, R. W. 1964 Radiation stress in water waves—a physical discussion with applications. *Deep Sea Res.* **11**, 529–562. (doi:10.1016/0011-7471(64)90001-4)
- 40 Constantin, A. & Varvaruca, E. 2011 Steady periodic water waves with constant vorticity: regularity and local bifurcation. *Arch. Ration. Mech. Anal.* **119**, 33–67. (doi:10.1007/s00205-010-0314-x)
- 41 Constantin, A. & Escher, J. 2004 Symmetry of steady periodic surface water waves with vorticity. *J. Fluid Mech.* **498**, 171–181. (doi:10.1017/S0022112003006773)
- 42 Constantin, A. & Escher, J. 2004 Symmetry of steady deep-water waves with vorticity. *Eur. J. Appl. Math.* **15**, 755–768. (doi:10.1017/S0956792504005777)
- 43 Constantin, A., Ehrnstrom, M. & Wahlen, E. 2007 Symmetry of steady periodic gravity water waves with vorticity. *Duke Math. J.* **140**, 591–603. (doi:10.1215/S0012-7094-07-14034-1)
- 44 Galvin, C. J. 1968 Breaker type classification on three laboratory beaches. *J. Geophys. Res.* **73**, 3651–3659. (doi:10.1029/JB073i012p03651)